UNIVERSITA' DEGLI STUDI DI VERONA

DEPARTMENT OF

NEUROSCIENCES, BIOMEDICINE AND MOVEMENT SCIENCES

GRADUATE SCHOOL OF

NATURAL SCIENCES AND ENGINEERING

DOCTORAL PROGRAM IN

NANOSCIENCE AND ADVANCED TECHNOLOGIES

Cycle

XXIX

TITLE OF THE DOCTORAL THESIS

"***INVESTIGATING THE EFFECT OF SUPERPARAMAGNETIC IRON OXIDE NANOPARTICLES ON HYPERPROLIFERATIVE CELLULAR MODEL DISEASE***"

S.S.D. BIO-16

Coordinator: Prof. Franco Tagliaro

Tutor: Dr. ssa Laura Calderan

Co-Tutor: Prof. Davide Prosperi

Doctoral Student: Dott./ssa Maria Rosaria Marinozzi

Investigating the effect of superparamagnetic iron oxide nanoparticles on hyperproliferative cellular model disease- Maria Rosaria Marinozzi
Tesi di Dottorato
Verona,
ISBN

Contents

Abstract 7

Introduction

I. Background 11

II. Adipose Tissue

II. I. General introduction to adipose tissue 12

II. II. Adipose tissue's pathology: Obesity 14

III. Nanotechnology and Nanomedicine

III.I. Introduction to nanomedicine 16

III.II. Nanoparticles for biomedical application 17

III.II.I. SPIONs as 'gold standard' in biomedicine 19

III.II.II. SPIONs as heat mediator for hyperthermia 20

IV. Assembling a nanoplatform

IV.I. Chemical Synthesis 22

IV.II. Surface modification 23

V. Aim of the work 24

VI. References 25

CHAPTER 1. Synthesis of efficient SPIONs for Thermotherapy

1.1. Introduction

1.1.1. Magnetic hyperthermia 31

1.1.2. Aim of the work 32

1.2.Materials and Methods

1.2.1. Reagents 33

1.2.2. Synthesis of iron-oleate complex 33

1.2.3. Synthesis of surfactant-coated spherical iron oxide nanoparticles (SIOs) 33

1.2.4. Snthesis of surfactant-coated polyhedral iron oxide nanoparticles (PIONs) with hyperthermic properties 34

1.2.5. Synthesis of nanocubic iron oxide nanoparticles (IONs) with hyperthermic properties 35

1.2.6. Polymer synthesis for water-phase transfer 35

1.2.7. Water phase transfer 36

1.2.8. Particles size and surface charge analysis 36

1.2.9. Iron quantification by ICP analysis 37

1.2.10. Hyperthermic efficiency of nanoparticles 37

1.2.11. Statistical Analysis 38

1.3. Results and Discussion

1.3.1. Synthesis and characterization of superparamagnetic iron oxide nanoparticles 39

1.3.2. Polymer synthesis 40

1.3.3. Water-phase transfer 41

1.3.4. Determination of the hyperthermic power of SPIONs in acqueos medium 45

1.4. Conclusions

47

1.5. References 48

Chapter 2 Application of Thermotherapy to adipose tissue

2.1. Introduction

2.1.1. Adipose Tissue Reduction 51

2.1.2. Aim of the work 53

2.2. Materials and Methods

2.2.1. Cell cultures 54

2.2.2. Cell viability Assay 54

2.2.3. Flow cytometry analysis of PIOs internalization 55

2.2.4. Confocal Laser Scanning Microscopy 55

2.2.5. SMHT treatment 56

2.2.6. qRT-PCR 56

2.2.7. Transmission Electron Microscopy 57

2.2.8. Oil Red O staining and intracellular triglyceride quantification 57

2.2.9. Glycerol analysis of release of fatty acid from adipocytes exposed to SMHT 58

2.3. Results and Discussion

2.3.1. PIONs toxicity in 3T3-L1 adipocytes cells 59

2.3.2. PIONs uptake in 3T3-L1 adipocytes cells 59

2.3.3. Impact of SMHT on intracellular distribution and cytotoxicity of PIOs in adipocytes 63

2.3.4. Lipolytic effect of SMHT in 3T3-L1 mature adipocytes 66

2.3.5. SMHT effects on intracellular metabolism of triglycerides in 3T3-L1 adipocytes 68

2.4. Conclusions 70

2.5. References 73

Appendix- Application of Thermotherapy to Glioblastoma

3.1. Introduction

3.1.1. Glioblastoma 76

3.1.2. SPIONs as contrast agents in MRI 77

3.1.3. SPIONs as theranostic agents 79

3.1.4. Targeting nanoparticles 79

3.1.5. GE11 Peptide 81

3.1.6. Aim of the work 83

3.2. Materials and Methods

3.2.1. Cell cultures 84

3.2.2. GE11 Solid-Phase Synthesis 84

3.3. Results and Discussion 87

3.4. Conclusions 89

3.5. References 90

3.6. Notes 91

General Conclusions 92

Abstract

The growing impact of nanotechnology in the field of medicine as a new potential clinical therapeutic agent requires the joint efforts of interdisciplinary research groups.

Numerous questions must be faced. The main issues to be considered involve the mechanisms of interaction with the cells before, during and after their adhesion and internalization, the degradation pathways, cytotoxicity and the therapeutic efficacy.

For these reasons, I attended to the construction of superparamagnetic iron oxide nanoparticles capable of providing compelling evidence of any of the above-described key factors. To assess the utility of these nanoparticles, I chose to treat obesity and glioblastoma as two hyperproliferative disease models, which affect millions of adult every year worldwide.

An attractive innovative possibility to approach the hyperproliferation can be envisaged in developing heating agents via magnetic nanoparticles. Thanks to their unique magnetic properties, superparamagnetic iron oxide nanoparticles now find large application as heating mediators for thermotherapy.

These nanoparticles need to fulfil several criteria in order to be used as therapeutic agents in humans, including nontoxicity, heating efficiency and sensitivity of detection resulting in a capability of the nanoparticles to be confined preferentially at the diseased site. It is common believed in fact that alternative factors, including opsonisation, macrophage-mediated transport and passive delivery in general, might strongly affect the targeting efficiency and final destiny of nanoparticles. Using magnetic nanoparticles coated with protein-targeting biomarkers overexpressed by targeted tissue may be provided these factors.

So the last step of the present work was focused on the construct of a peptide-nanoconjugate to perform an accurate study of nanoparticle-membrane receptor in vivo.

In summary, the general scope of this thesis was to develop an efficient nanoparticle for the investigation of the effect of thermotherapy mediated by magnetic nanoparticles on two hyperproliferative diseases.

Several issues including nanoparticles synthesis, bio-functionalization, toxicity and the use as therapeutic agents have been thoroughly examinated and optimized. By taking advantage of the interdisciplinary view offered by synergistic chemical,

physical and biochemical approaches, I have designed a new nano-system suitable to explore new frontiers in the therapy of the hyperproliferative diseases.

Of course, the clinical application in human treatments is the final goal of this and its related research. However, to reach such objective is necessary not only to design a suitable system for practical use, but also to assess and optimize the essential characteristics for specific effects such as safety, capability to get to the specific target, to provide useful signal amplification and to avoid the immunogenic system.

Introduction

I. Background

Obesity and tumours have become the two major health threats in industrialized countries. In most cases they are strictly correlated and they influence each other. Among all kinds of tumour one of the most aggressive and with a poor prognosis is glioblastoma.

Currently, for these pathologies there is no an efficient cure and only very limited progress has been made in the control of the diseases course and of the ill-fated prognosis. Only in few cases it is possible to perform surgery and often it is not conclusive. Thus, the need for effective therapies is great.

In recent years, nanoparticles have been the protagonists in biomedical research and in some cases they have been clinical applications. Researchers and clinicians use the unique chemical/ physical properties of nanomaterials for research investigation, for diagnosis and treatment of several otherwise untreatable diseases and for improving the performance of many treatments.

II. Adipose Tissue

II.I. General introduction to adipose tissue

The perception of adipose tissue has dramatically changed with the increase in the incidence of obesity and obesity-related comorbidities. Adipose tissue is increasingly being considered not simply as fat store, but as a vital and complex endocrine organ [1]. It shows protective, mechanical and trophic functions. Moreover, data support a potential role of adipose tissue in the evolution of the human brain, as well as in myocardial regeneration and repair [2].

In humans, adipose tissue is located beneath the skin (subcutaneous adipose tissue), around internal organs (visceral adipose tissue), in bone marrow (yellow bone marrow), and in breast tissue.

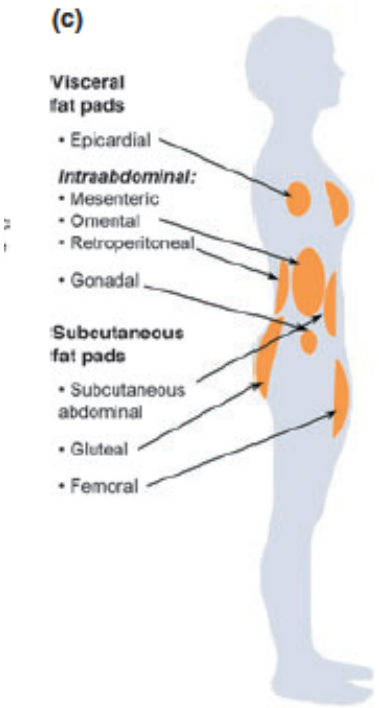

Figure 1: Localization of the major white adipose tissue in human body [5].

Most adipose tissue consists of several cell types including adipocytes and the stromal vascular fraction (SVF), comprising preadipocytes, fibroblasts, vascular endothelial cells and a variety of immune cells all interspaced by a cytokine-rich extracellular matrix and blood vessels [3].

Three types of adipose tissue exist in humans, namely the brown (or plurivacuolar), the beige and the most common white (or monovacuolar) adipose tissue [4]. The beige adipose tissue is formed by beige cells which are very similar to white cells having a low basal expression of UCP1, but they respond to cAMP stimulation with high UCP1 expression, reaching similar absolute levels to the brown adipocytes [6].

The brown fat cells are related to thermogenesis. They use the chemical energy of lipids and glucose to produce heat. This process is mediated by the expression of the mitochondrial uncoupling protein 1 (UCP1), causing the thermogenesis via mitochondrial uncoupling of oxidative phosphorylation of free fatty acids [7].

Finally, the white adipose tissue is composed by highly metabolically active cells containing a single large lipid droplet anchored by collagen fibers forcing the nucleus to be squeezed into a thin rim at the periphery. Because of their metabolic function, these cells can directly affect the physiologic processes in neighbouring and distant cells by activating endocrine and paracrine pathways through an increase in secretion.

The most important secretions are fatty acids. In addition, several other lipid moieties are released by fat cells; these include prostanoids, cholesterol and retinol. Also a wide range of highly diverse protein factor and signalling molecules, called adipokines are released from adipose tissue with important roles in the regulation of angiogenesis, blood pressure, glucose homeostasis, lipid metabolism vascular haemostasis and inflammatory respons [8-9] (Figure 2).

So, far from being an inert tissue, adipose tissue has been shown to be a super-dynamic organ with several sophisticated functions influenced by its developmental origins but also by its interaction with the other organs.

Table 1 | Factors secreted by adipose tissue

Category	Factors
Lipid metabolism	Apolipoprotein E,[149] free fatty acids,[150] glycerol, lipoprotein lipase[151]
Steroid hormones	Estradiol,[152] estrone, testosterone
Growth factors and cytokines[153]	IL-1β, IL-6, insulin-like growth factor I, leptin,[154] nerve growth factor, tumor necrosis factor, vascular endothelial growth factor
Vasoactive factors	Adipocyte-derived relaxing factor,[90] angiotensinogen, angiotensin II, atrial natriuretic factor,[155] monobutyrin[156]
Eicosanoids	Prostacyclin (prostaglandin I2), prostaglandin E2, prostaglandin F2α
Complement system[157]	Complement factors B, C, C1q, C3, and D[158]
Binding proteins	Insulin-like growth factor mRNA-binding proteins, retinol-binding protein,[159] tumor necrosis factor receptors[160]
Extracellular-matrix proteins	C–C motif chemokine 2 (monocyte chemotactic protein 1)[161]
Others	Adiponectin,[162] angiopoietin-related protein 4, apelin,[163] cholesterol ester transfer protein, haptoglobin, intelectin-1 (omentin),[164] irisin,[12] lysophosphatidic acid,[165] metallothionen,[166] plasminogen activator inhibitor 1,[167] resistin,[168] visfatin (nicotinamide phosphoribosyltransferase)[55]

Figure 2: Factor secreted by adipose tissue [3].

II.II. Adipose tissue's pathology: Obesity

Obesity represents a relevant dangerous disease to the public's health industrialized countries. It is considered a high threat because it represents the major risk factor in the etiopathology of several other diseases (cardiovascular disease, hypertension, hyperlipidemia, diabetes mellitus, stroke and cancer) [10] and it is characterized by the expansion of adipose tissue induced by an excessive food intake over energy expenditure. A deeply knowledge of the mechanisms involved in the homeostasis of adipose tissue must be faced for developing new efficient therapies for obesity.

"The growth of adipose tissue could be either due to an increase in the volume of adipocytes (adipose hypertrophy) or to an excess number of adipocytes (hyperplasia)" (Figure 3) [11]. The hyperplasia and hypertrophy result in a dysregulation in circulating hormones affecting systemic energy balance.

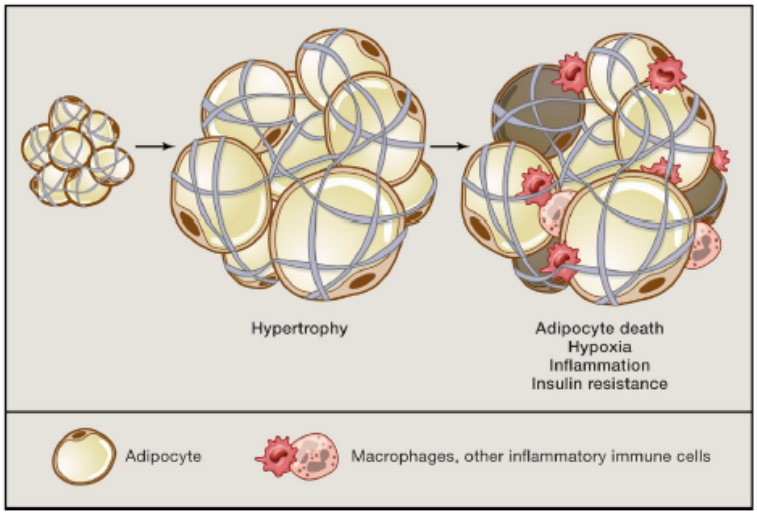

Figure 3: during overnutrition adipocytes increase in size until further expansion becomes limited by the matrix, which undergoes fibrotic changes [4].

In the adipose tissue of obese patients increase the concentration of leptin and decrease the production of adipokines suggesting that it could be correlated with any mitogenic stimuli, anti-apoptotic and pro-angiogenic effects, enhancing the cancer risk [12]. Also an alteration in vascular tissue development and hypoxia associated with macrophage infiltration is essential during expandibility of adipose tissue. As a consequence, the dysfunction of adipose tissue is a critical predictor of metabolic disorders, such as insulin resistance, hyperinsulinemia, elevated triglyceride levels, low HDL-cholesterol and hypertension [13,14].

It is now clear how much is important to deeply known the mechanism involved in obesity because adipocytes exert a profound influence in neighbouring and distant tissues by activating endocrine and paracrine pathways through an increase in secretion, resulting in a real crosstalk with other tissues (Figure 4).

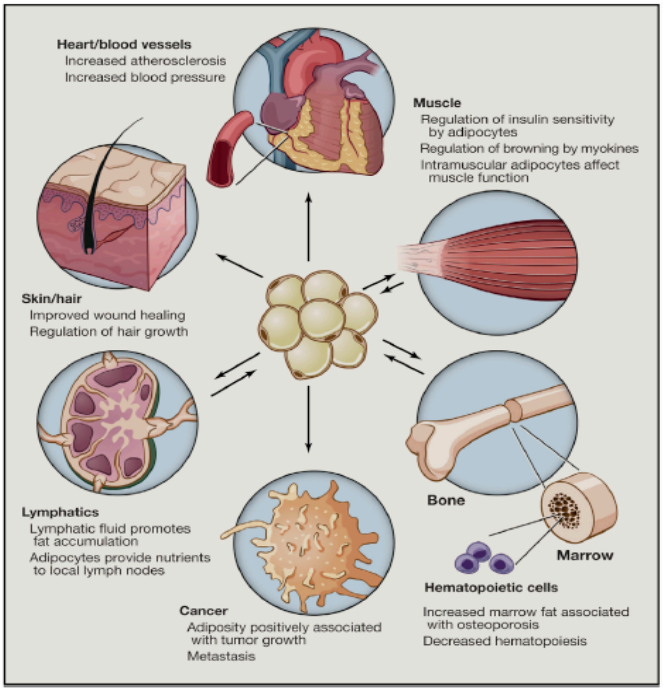

Figure 4: adipose tissue crosstalk with other tissues [4].

Another important criterion in predicting diseases associated with obesity is the regional body distribution. "The regional body distribution of adipose tissue is at least as important than the total amount of body fat" [15]. For instance, accumulation of visceral adipose tissue is associated with insulin resistance, metabolic syndrome and related cardiovascular complications. Conversely, peripheral subcutaneous adipose tissue exhibits an independent antiatherogenic effect, which is not related to the obesity-pathologies. A relative simple technique to evaluate the total and regional adiposity in individual involves a study of the whole body with a scan densitometer [16].

As currently the reduction of adipose tissue is obtained by the reduction/inhibition of food intake through pharmacological stimulation of the central nervous system or by blocking the absorption of lipids in the gut with however many side effects, a directly targeting of the adipose tissue could be an innovative strategy for obesity treatment.

III. Nanotechnology and Nanomedicine

III.I. Introduction to nanomedicine

The ideas and concepts behind nanoscience and nanotechnology started with the physicist Richard Feynman on December 29, 1959, at the American Physical Society meeting at the California Institute of Technology with a talk entitled *"There's Plenty of Room at the Bottom"* (Figure 1) describing a process in which scientists would be able to manipulate and control individual atoms and molecules: "*A biological system can be exceedingly small. Many of the cells are very tiny, but they are very active; they manufacture various substances; they walk around; they wiggle; and they do all kinds of marvellous things- all on the very small scale. Also they store information. Consider the possibility that we too can make a thing very small, which does what we want- that we can manufacture an object at that level!*".

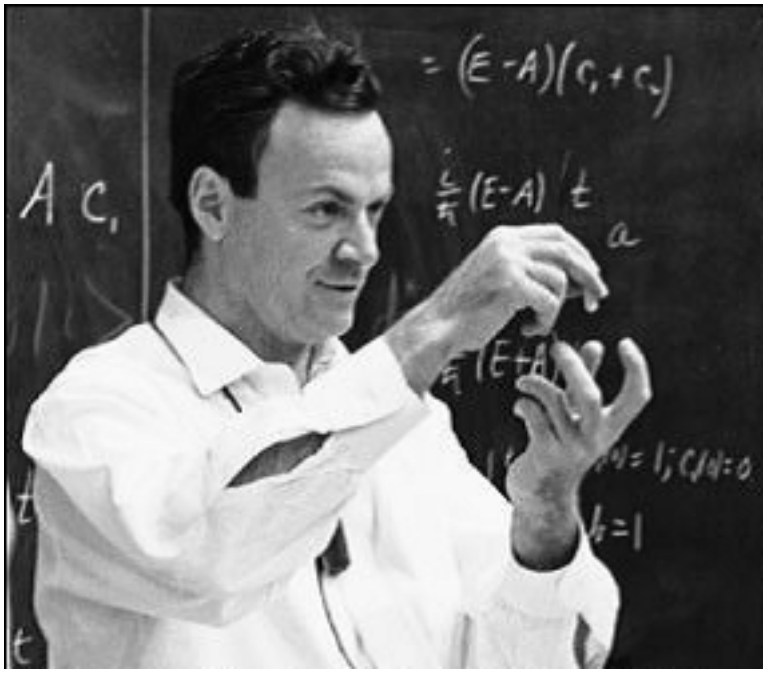

Figure 5: Richard Feynman

At the present, nanotechnology is defined by the National Institutes of Health in USA as "the understanding and control of matter at dimensions of roughly 1 to 100 nanometers". At the nanoscale, the nanosystems own unique chemical, physical, and biological properties and are also very similar in scale to biological molecules and systems, therefore they are potentially useful for biomedical applications.

The applications of nanotechnology to the biological systems have recently been referred to as "Nano medicine" by the National Institutes of Health in USA [17]. In particular, nanomedicine exploits the properties of nanomaterials for the diagnosis and treatment of diseases at the molecular level. Nanomaterials are now being designed to aid the transport of diagnostic or therapeutic agents through biological barriers, to gain access to specific functions, to mediate molecular interactions, and to detect molecular changes in a sensitive and highly efficient manner. Nano-scientists created a new generation of drug delivery vehicles, contrast agents and diagnostic devices, some of which are currently undergoing clinical trials or have been approved by the Food and Drug Administration (FDA) for use in humans, others are in the proof-of-concept stage in research laboratories (Figure 2).

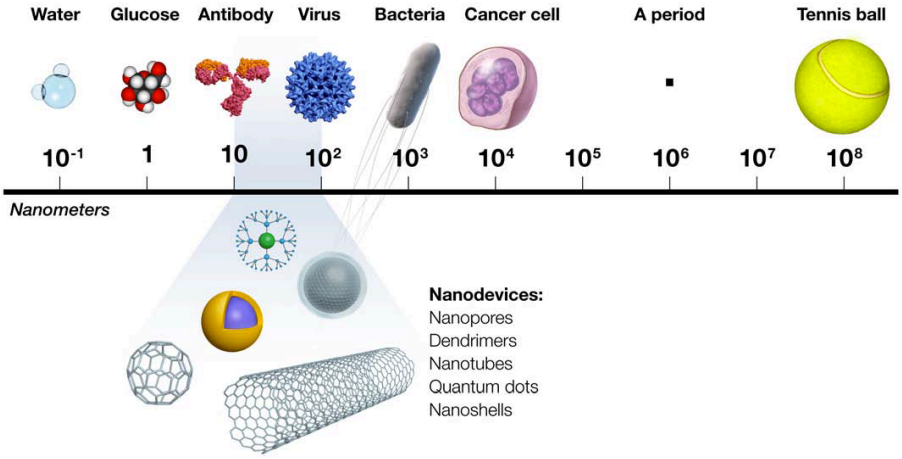

Figure 6: The size of things. Nanoscale devices are one hundred to ten thousand times smaller than human cells [18].

III.II. Nanoparticles for biomedical application

In the field of nanomedicine particular attention is given to the nanoparticles: particles with a well-defined chemical structure, self-organization and composition with sizes ranging between 1 to 100 nm [19]. They own tunable optical, electronic, magnetic and biological properties. In addition they can be engineered to have different sizes, shapes, chemical compositions, surface chemical characteristics, and hollow or solid structures. Nanoparticles generally consist of metal atoms, non-metal atoms, or a mixture of metal and non-metal atoms. The surface of nanomaterials is usually coated with polymers or bio recognition molecules to achieve an improved biocompatibility and selective binding with biological molecules and also to avoid

physiological defence systems (opsonization, renal clearance, etc) to optimize biodistribution.

Several nanoparticles are in the clinical trial phase or have already been approved by the FDA for use in humans; many others are in the pre-clinical phase [20-21]. Often they are designed to treat pathologies otherwise non-curable and are intended for use either as drug carriers or as contrast agents for molecular imaging.

Moreover these nanovehicles can also be coated with polymers, such as *in primis* with polyethylene glycol, to increase their half-life in the blood circulation, to prevent opsonins for adhering to the nanomaterial surface, and to reduce the rapid metabolism of the nanoparticulate before they reach the target tissue and avoiding their accumulation in other tissues.

Another important approach is to minimize the kidney clearance. In this sense is fundamental to modify the physico-chemical properties of the nanoparticles to avoid ultrafiltration and secretion in renal nephron.

Moreover the specific targeting allow minimizing side effects by preventing the nonspecific uptake of therapeutic agents from healthy tissues [22]. In addition, the high ratio of surface area to volume of nanoparticles favours high surface loading of therapeutic agents. Possible applications include drug delivery, cell targeting, multi modal diagnostic imaging (MRI, PET, TAC) contrast enhancement, gene therapy, biomarker identification, targeted hyperthermia and many others [23].

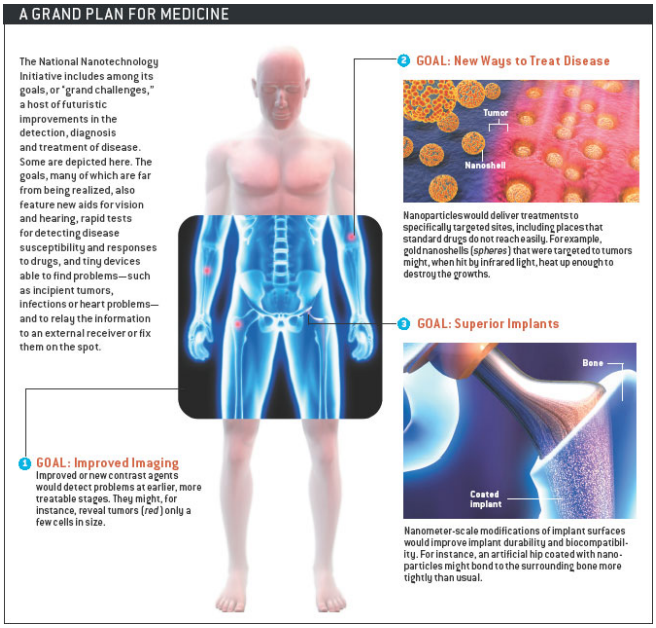

Figure 7: Potential of nanomedicine [24].

III.II.I. SPIONs as 'gold standard' in biomedicine

Among all kinds of nanoparticles, superparamagnetic iron oxide nanoparticles (SPIONs) have attracted attention as interesting cargos for biomedical application because of their potential usefulness in oncological medicine [25] as contrast agents in magnetic resonance imaging and as colloidal mediators for cancer magnetic hyperthermia [26] thanks to their physic properties [27], biocompatibility [28], biodegradability [29] and facile synthesis [30]. In fact, SPIONs exhibit unique physical and chemical properties summarized as superparamagnetic behaviour that dramatically changes some of the magnetic properties [31]. Moreover, FDA has already approved SPIONs for use in humans; in fact the release of the iron ions upon dissolution can be assimilated by the body *via* physiological processes in their own metabolism. However, it remains crucial to monitor their use as therapeutic agents for repeated and chronic treatments [32].

Because of their very small size, SPIONs can be administered by alternative routes to injection, including inhalation [33], ingestion [34], and skin penetration [35]. It can be assumed that they are able to interact with intracellular structures and modulate the physiology of the cell with external, non-invasive and harmless stimuli.

Typically, SPIONs are composed by a magnetic core providing the specific properties and by a biocompatible coating that provides ample functional groups for conjugation of additional therapeutic moieties (Figure 3).

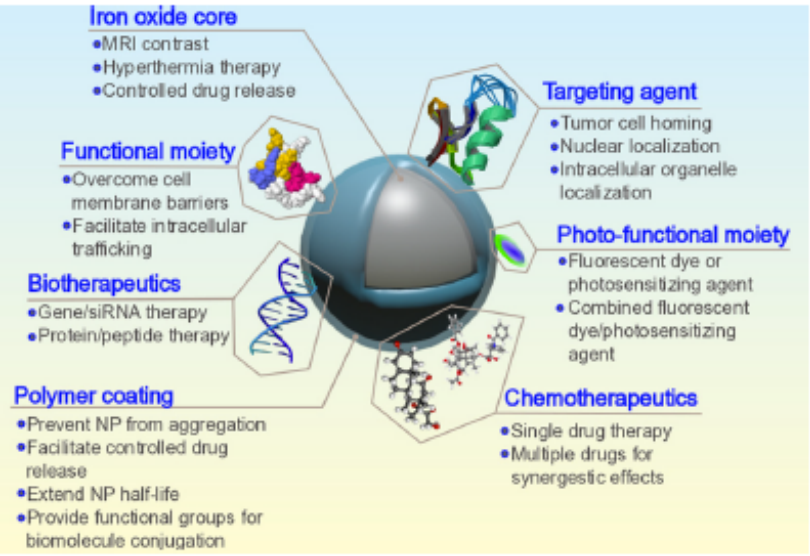

Figure 8: schematic illustration of a full-suite SPION. The magnetic core serves as MRI contrast and as heat source for hyperthermia instead the polymer coating increases biocompatibility, reduce the uptake by immune system and allows the functionalization with antibody or chemotherapeutics [26].

III.II.II. SPIONs as heat mediators for hyperthermia

A very innovative application of SPIONs is thermotherapy, which is considered a supplementary treatment associated with chemotherapy, radiotherapy and surgery [36]. In fact thanks to their superparamagnetic behaviour, SPIONs are able to produce heat when subjected to an alternating magnetic field (AMF) [37]. The origin of the magnetic properties lies in the orbital and spin motions of electrons, whose spin and angular momentum are associated with a magnetic moment. So, applying an external magnetic field operating at a specific frequency and power based on the SPIONs properties causes heat by hysteresis loss, Nèel relaxation, and induced eddy currents. Therefore they became available heat mediator exhibiting a sufficient heating capacity to achieve satisfactory temperatures *in vivo* without the addition of functional moieties. The amount of heat generated depends on the nature of magnetic material and of magnetic field, the frequency of oscillation and the cooling capacity of the blood flow in the tumour [38-39].

It is thought that, in such a temperature range, the function of many structural and enzymatic proteins within cells is modified, which in turn alters cell growth and differentiation and can induce apoptosis. Cancer cells are sensitive to temperature increase and are killed when the temperature rises above 43 °C, whereas the normal cells can survive at higher temperature values. So, a novel hyperthermia route for tumours would consist of concentrating SPIONs around and inside the tumour tissue and making them heat through energy absorption from an external alternating magnetic field (Figure 5).

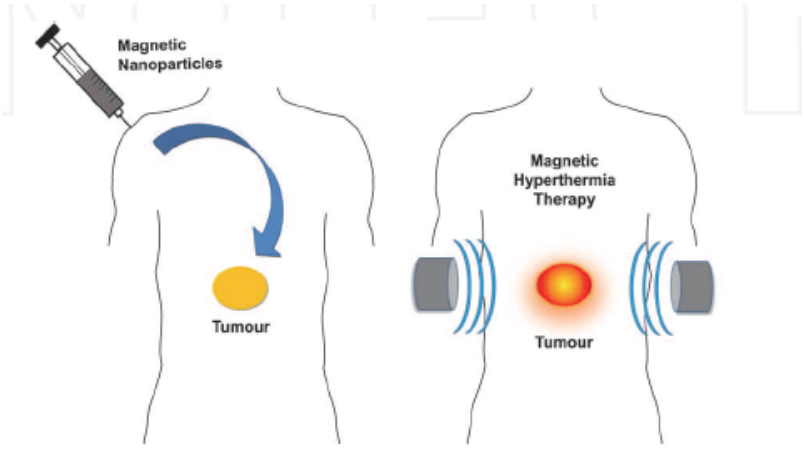

Figure 9: general procedure for thermotherapy. SPIONs were firstly injected into the human body and then an externally applied alternating magnetic field induced the hyperthermia [40].

Superparamagnetic iron oxide nanoparticles-mediated magnetic hyperthermia (SMHT) seems to have advantages over conventional hyperthermic approaches because heat-generating nanoparticles could be prepared in colloidal suspensions suitable for fast injection avoiding the need for macroscopic implants. In addition, their distribution could potentially be controlled by different targeting strategies, and the particles could be made small enough to cross the biological barriers and generate heat very close to target tissue reducing side effects compared to traditional treatments. The SMHT could be performed according three strategies: arterial embolization hyperthermia (AEH), direct injection hyperthermia (DIH), and intracellular hyperthermia (IH). Their use appears as the most promising cancer hyperthermia therapy in particular because of the better temperature homogeneity.

With respect to the patient's comfort, it was found that the product *Hv* (where H is the amplitude and v the frequency of the AC magnetic field) should be lower than 4.85×10^8 A m^{-1} s^{-1} for a treatment duration of one hour [41]. Moreover, the frequency has to be superior to 50 kHz for avoiding neuromuscular electro stimulation and lower than 10 MHz for appropriate penetration depth of the rf-field [42].

A few studies in humans using iron oxide nanoparticles as mediators of magnetic hyperthermia are ongoing for the treatment of colon cancer [43], prostate cancer [44] and for the reduction of bone tumours [45], with promising clinical outcomes. Clinical results showed that the combination of radiation therapy and hyperthermia conducted to a substantial therapeutic improvement [46]. Very recently, it has been demonstrated that improved efficiency could be obtained combining AMF and near-infrared laser irradiation [47].

IV. Assembling a nanoplatform

IV.I. Chemical synthesis

As the superparamagnetic behaviour depends on several parameters, it's relevant to carefully evaluate the chemical variability to realize efficient SPIONs. In fact, the final size, composition, shape (spherical, rod-like, star-like, wires, octahedral, cubic etc.) of SPIONs depend on the salt and surfactant additives, reactant concentrations, reaction temperatures and solvent conditions used during their synthesis.

Preparing monodisperse SPIONs requires the separation of nucleation step from the growth of nanocrystals. The "burst nucleation" event occurs at a critical supersaturation of the monomer concentration. The resulting nuclei grow at the same rate, obtaining monodisperse nanocrystals. Nevertheless these nanocrystals agglomerate rapidly to minimize their surface energy. Thus, a suitable capping agent is necessary to stabilize these nanoparticles and prevent them by forming aggregates.

Numerous synthetic methods are used to synthesize SPIONs [48-55].

Among all these methods the thermal decomposition is the most used thanks to the possibility of obtaining SPIONs with a better-controlled size and morphology. A typical thermal decomposition requires the presence of a metal complex and a surfactant in an organic solvent with a high-boiling point. In the reaction, the precursors are heated up from a homogeneous mixture. In the heating up procedure, all the precursors are mixed and heated, so magnetic nanoparticles are made by tailoring reaction temperature and precursors concentration. Oleic acid is used as surfactant for nanoparticle stabilization and for the control of nanoparticle size and morphology. The metal precursors are usually metal acetylacetonates and metal oleates. At the end is obtained are obtained size-controlled monodisperse Fe_3O_4 nanoparticles (Figure 13).

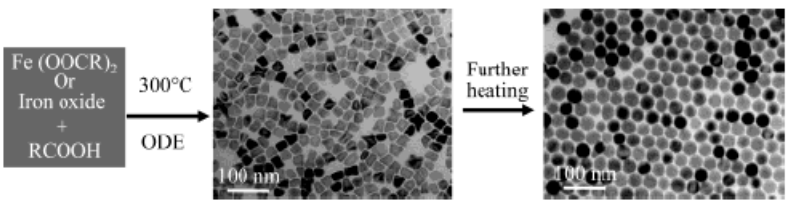

Figure 10: schematic illustration of the formation of Fe_3O_4 nanocrystals [56].

IV.II. Surface modification

Obtaining stable, biocompatible and storable SPIONs requires modifying the SPIONs surface. In fact in the absence of any surface coating, SPIONs have hydrophobic surfaces with a large surface area to volume ratio. Due to colloidal interactions between the particles, these particles agglomerate and form large clusters resulting in aggregation and precipitation. Stabilizers such as surfactants or polymers are usually added at the time of preparation to prevent aggregation of the nanoscale particulate leading to a hydrophobic surface. To make these nanoparticles biocompatible their surface needs to be functionalized with a surfactant addition. Surfactant addition is achieved by means of the adsorption of amphiphilic molecules that contain both a hydrophobic segment and a hydrophilic component. The hydrophobic segment forms a double layer structure with the original hydrocarbon chain anchored to the nanoparticle surface, while the hydrophilic groups are exposed to the outer layer of the nanoparticle, conferring it water solubility. This bifunctional surfactant has one functional group available for binding to the nanoparticle surface tightly via a strong chemical bond and the second functional group at the other end has a polar character so that the nanoparticle can be dispersed in water or be conjugated to a further molecule.

There are various kinds of materials that can be chosen for coating nanoparticles: Polymer coating materials, including lipids, proteins, dendrimers, gelatin, dextran, chitosan and PEG [57].

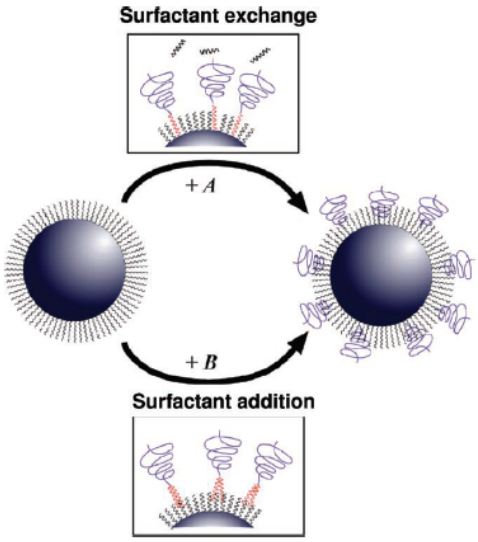

Figure 11: strategies for SPIONs surface modifation [58].

V. Aim of the work

Currently there is no an efficient treatment for the "hyper-proliferative" diseases and though research remains to be done into the development of accurate therapies.

The aim of my PhD project was to take advantage of the efficacy of the magnetic hyperthermia mediated by super iron oxide nanoparticles (SPIONs) to enhance the targeting and the therapeutic effect of the thermotherapy against two "hyper-proliferative" disease cellular models: obesity and glioblastoma.

In fact, magnetic hyperthermia mediated by magnetic nanoparticles represents a new promising approach, particularly for its ability to reach the targeted tissue and to modify the cellular behaviour avoiding side effects.

Therefore, my PhD thesis included three chapters, in which I have described in more details the nanoparticles and their possible applications.

VI. References

[1] Marti, A., et al., 'Obese' protein slims mice. *Science* 269 (1995) 475-476.

[2] Aiello, L.C., et al. The expensive-tissue hypothesis-the brain and the digestive system in human and primate evolution. *Curr. Anthropol.* 36 (1995) 199-221.

[3] Hassan, M., et al., Adipose tissue: friend or foe?. *Nat. Rev. Cardiol.* 9 (2012) 689-702.

[4] Rosen, E.D., et al., What we talk when we talk about *Fat. Cell* 156 (2004) 20–44.

[5] Wronska, A., et al., Structural and biochemical characteristics of various adipose tissue depots. *Acta Physiol* 205 (2012) 194-208.

[6] Wu, J., et al. Beige adipocytes are a distinct type of thermogenic fat cell in mouse and human. *Cell* 150 (2012) 366-376.

[7] Lidell, M. E., et al., Brown adipose tissue-a new role in humans?. *Nat.Rev. Endocrinol.* 6 (2010) 319-325.

[8] Chu, F., et al., Plasma insulin, leptin, and soluble TNF receptors levels in relation to obesity-related atherogenic and thrombogenic cardiovascular disease risk factors among men. *Atherosclerosis* 157 (2001) 495–503.

[9] Hajer, G. R., et al., Adipose tissue dysfunction in obesity, diabetes, and vascular diseases. *Eur. Heart J.* 29 (2008) 2959–2971.

[10] Alappat, L., et al., Curcumin and Obesity: evidence and mechanisms, *Nutr. Rev.* 68 (2010) 729-738.

[11] Rutkowski, J. M., et al., The cell biology of fat expansion. *J. Cell Biol.* 208 (2015) 501–512.

[12] Renehan, A. G., et al., Adiposity and cancer risk: new mechanistic insights from epidemiology. *Nat. Rev. Cancer* 15 (2015) 484–498.

[13] Arner, E., et al., Adipocyte turnover: relevance to human adipose tissue morphology. *Diabetes* 59 (2010) 105–109.

[14] Jo, J., et al., *PLoS Comput. Biol. 5* (2009) e1000324. Doi: 10.1371/journal.pcbi.1000324.

[15] Tchernof, A., et al., Pathophysiology of human visceral obesity: an update, *Physiol Rev.* 93 (2013) 359-404.

[16] Taylor, R.W., et al., Evaluation of waist circumference, waist-to-hip ratio, and the conicity index as screening tools for high trunk fat mass, as measured by dual-energy X-ray absorptiometry, in children aged 3-19 y. *Am J Clin Nutr* 72 (2000) 490-495.

[17] Kim, B.Y.S., et al., Nanomedicine. *N. Engl. J. Med.*, 363 (2010), 2434-2443.

[18] Understanding nanotechnology, NCI Alliance for Nanotechnology in Cancer. https://nano.cancer.gov/learn/understanding/.

[19] Freitas, R.A, What is nanomedicine?, *Nanomedicine* 1 (2005) 2-9.

[20] Peer, D., et al., Nanocarriers as an emerging platform for cancer therapy, *Nat. Nanotech.* 2 (2007) 751-760.

[21] McCarthy, T. D., et al., Dendrimers as drugs: discovery and preclinical and clinical development of dendrimer-based microbicides for HIV and STI prevention, *Mol. Pharm.* 2 (2005) 312-318.

[22] Alexis, F., et al., Factor affecting the clearance and biodistribution of polymeric nanoparticles, *Mol. Pharm.* 5 (2008), 505-515.

[23] Ferrari, M., Cancer nanotechnology: opportunities and challenges, *Nat. Rev. Cancer* 5 (2005) 161-171.

[24] Alivisatos, A. P., Less is more in Medicine, *Sci. Am.*, 2001, 67-73.

[25] Mornet, S., et al., Magnetic nanoparticle design for medical diagnosis and therapy. *J. Mater. Chem.* 14 (2004) 2161-2175.

[26] Revia, R. A., et al., Magnetite nanoparticles for cancer diagnosis, treatment, and treatment monitoring: recent advances. *Mater. Today* 19 (2016) 157-168.

[27] Goya, G. F., et al., Static and dynamic magnetic properties of spherical magnetite nanoparticles, *J. Appl. Phys.* 94 (2003) 3520-3528.

[28] Sun, C., et al., PEG-mediated synthesis of highly dispersive multifunctional Superparamagnetic nanoparticles: their physicochemical properties and function in vivo. *ACS Nano* 4 (2010) 2402-2410.

[29] Weissleder, R., et al., Superparamagnetic iron oxide: pharmacokinetics and toxicity. *Am. J. Roetengenol.* 152 (1989) 167-173.

[30] Sun, C., et al., Magnetic nanoparticles in MR imaging and Drug Delivery. *Adv. Drug Del. Rev.* 60 (2008) 1252-1265.

[31] Colombo, M., et al., Biological applications of magnetic nanoparticles. *Chem. Soc. Rev* 41 (2012) 4306–4334.

[32] Mahmoudi, M., et al., Assessing the in vitro and in vivo toxicity of superparamagnetic iron oxide nanoparticles. *Chem. Rev.* 112 (2012) 2323–2338.

[33] Verma, N. K., et al., Magnetic core-shell nanoparticles for drug delivery by nebulization. *J. Nanobiotechnol.* 11 (2013) 1.

[34] Chamorro, S., et al., Safety assessment of chronic oral exposure to iron oxide nanoparticles. *Nanotechnology* 26 (2015) 205101.

[35] Santini, B., et al., Cream formulation impact on topical administration of engineered colloidal nanoparticles. *Plos One* 10 (2015) e0126366.

[36] Shellman, Y., et al., Hyperthermia induces endoplasmic reticulum-mediated apoptosis in melanoma and non-melanoma skin cancer cells. *J. Invest. Dermatol.*, 128 (2008), 949-956.

[37] Dubois, J. B., et al., Hyperthermia: principles, techniques. Current role in the treatment of cancer. *Bull. Cancer Radiother.* 82 (1995) 207-224.

[38] Jordan, A., et al., Inductive heating of ferrimagnetic particles and magnetic fluids: physical evaluation of their potential for hyperthermia. *Int. J. Hyperthermia* 9 (1993) 51–68.

[39] Boubeta, C. M., et al., Learning from Nature to Improve the Heat Generation of Iron-Oxide Nanoparticles for Magnetic Hyperthermia Applications. *Sci. Rep.* 3 (2013) 1652.

[40] Andrade, A., et al., Coating Nanomagnetic Particles for Biomedical Applications, INTECH Open Access Publisher, 2011.

[41] Andrä, W., in Magnetism in Medicine: A Handbook. ed. W. Andrä, and H. Nowak, Wiley-VCH, Berlin, 1998, 455.

[42] Hill, D. A., Further study of human whole-body radiofrequency absorption rates. *Bioelectromagnetics* 6 (1985) 33-40.

[43] Mannucci, S., et al., Magnetic nanoparticles from *Magnetospirillum Gryphiswaldense* increase the efficacy of thermotherapy in a model of colon carcinoma. *PLoS One* 9 (2014) e108959.

[44] Johannsen, M., et al., Thermotherapy of prostate cancer using magnetic nanoparticles: feasibility, imaging, and three-dimensional temperature distribution. *Eur. Urol.* 52 (2007) 1653–1662.

[45] Matsumine, A., et al., Novel hyperthermia for metastatic bone tumors with magnetic materials by generating an alternating electromagnetic field. *Clin. Exp. Metastasis* 24 (2007) 191–200.

[46] Maier-Hauff, K., et al., Intracranial thermotherapy using magnetic nanoparticles combined with external beam radiotherapy: results of a feasibility study on patients with glioblastoma multiforme. *J. Neuro-oncol.* 81 (2007) 53–60.

[47] Espinosa, A., et al., The duality of iron oxide nanoparticles in cancer therapy: amplification of heating efficiency by magnetic hyperthermia and photothermal bimodal treatment. *ACS Nano* 10 (2016) 2436–2446.

[48] Hofmann, A., et al., Highly modisperse water-dispersable iron oxide nanoparticles for biomedical applications, *J. Mater. Chem.* 20 (2010) 7842-7853.

[49] Dacoata, G. M., et al., Synthesis and characterization of some iron oxide by sol-gel method. *J. Solid State Chem.* 113 (1994) 406-412.

[50] Deng, Y., et al., Preparation of magnetic polymer particles via inverse microemulsion polymerization process, *J. Magn. Magn. Mater.* 257 (2003) 69-78.

[51] Mukh-Qasem, R. A., et al., Sonochemical synthesis of stable hydrosol of Fe3O4 nanoparticles, *J. Colloid Interface Sci.* 284 (2005) 489-494.

[52] Chen, D., et al., Hydrothermal synthesis and characterization of nanocrystalline Fe3O4 powders, *Mater.Res. Bull.* 33 (1998) 1015-1021.

[53] Hyeon, T., et al., Synthesis of highly crystalline and monodisperse maghemite nanocrystallites without a size-selection process, *J. Am. Chem. Soc.* 123 (2001) 12798-12801.

[54] Basak, S., et al., Electrospray of ionic precursor solution to synthesize iron oxide nanoparticles: modified scaling law, *Chem. Eng. Sci.* 62 (2007) 1263-1268.

[55] Veintemillas-Verdaguer, S., et al., Continuous production of γ- Fe2O3 ultrafine powders by laser pyrolysis, *Mater. Lett.* 35 (1998) 227-231.

[56] Jana, N. R., et al., Size- and Shape-Controlled Magnetic (Cr, Mn, Fe, Co, Ni) Oxide Nanocrystals via a Simple and General Approach, *Chem. Mater* 16 (2004) 3931-3935.

[57] Lu, A. H., et al., Magnetic nanoparticles: synthesis, protection, functionalization and application. *Angew. Chem. Int. Ed.* 46 (2007) 1222-1244.

[58] Hao, R., et al., Synthesis, functionalization, and biomedical applications of multifunctional magnetic nanoparticles, *Adv. Mater.* 22 (2010) 2729-2742.

Chapter 1

Synthesis of efficient SPIONs for Thermotherapy

1.1. Introduction

1.1.1. Magnetic hyperthermia

Since of the pioneering work of Gilchrist et al. [1] the pursuit of innovative, multifunctional, efficient and safer SPIONs for magnetic hyperthermia represents a current challenge. Magnetic hyperthermia is based on the generation of heat *via* an alternating magnetic field (AMF) exploiting SPIONs as heating *foci*. In fact applying a specific AMF based on the SPIONs formulation causes the SPIONs to heat because SPIONs are able to convert electromagnetic energy into heat by hysteresis loss, Nèel relaxation, and induced eddy currents [2].

The heating ability of SPIONs subjected to an AMF is expressed as Specific Absorption Rate (SAR). SAR measures the rate at which energy is absorbed per unit mass of iron [3]. SAR values are influenced by the structure and the composition of the nanoparticles as well as by the concentration and the size of the nanoparticles. Moreover SAR changes (nanoparticles being equal) with the frequency and the amplitude of the magnetic field applied during the measurements [4].

Thus, as exists physical limitation in hyperthermia application [5] it is of great importance to develop a SPION able to induce hyperthermia with maximum efficiency and minimum toxicity.

1.1.2. Aim of the work

SAR values strongly depend on the chemical structure of the SPIONs. In order to reach the greater temperature with the minimum particles concentration is necessary to optimize the synthesis of the SPIONs as heating mediator avoiding toxicity and side effects.

Therefore, in this chapter I present the synthesis, characterization and the study of the heating power of three different kinds of SPIONs specifically designed as magnetic fluid hyperthermia heat mediators. Starting from an iron-oleate complex we synthesized two different kinds of SPIONs with few modifications in the synthetic approach. In this way we obtained two different nanoparticles: spherical iron oxide nanoparticles (SIOs) and polyhedral oxide nanoparticles (PIONs).

The first step study was focused on the heating ability of these two different kinds of nanoparticles to choose the more efficient for the second step *in vitro* in adipocytes.

Alternatevely for the second study we decided to change the synthetic procedure of SPIONs realizing iron oxide nanocubes (IONs) as more efficient heat mediator for hyperthermia treatment in glioblastoma.

1.2. Materials and Methods

1.2.1. Reagents

All reageants and solvents were of analytical grade and were used without any further purification. Water was deionized and ultrafiltered by a Milli-Q apparatus (Millipore Corporation, Billerica, MA).

For the spheric and polyhedral iron oxide nanoparticles: iron chloride (98%), sodium-oleate (95%), 1-octadecene (90%), oleic acid (90%), poly- (isobutylene-alt-maleic anhydride) (85%) ($M_w \approx 6000$ g mol^{-1} corresponding to roughly 20 mmol of monomer units per polymer chain), dodecylamine (98%), tetrahydrofurane anhydrous 99.9%), dimethyl sulfoxide, ethanol, hexane, acetone and chloroform were purchased from Sigma-Aldrich.

For the nanocubic iron oxide nanoparticles: Iron (III) acetylacetonate (99%), decanoic acid (99%), poly-(maleic anhydride alt-1-octadecene) and dibenzyl ether (99%) were purchased from Sigma-Aldrich.

1.2.2. Synthesis of iron-oleate complex

The iron-oleate complex was prepared by reacting iron chlorides and sodium oleate according to Park et al. [6]. Briefly, 1.8 g of iron chloride ($FeCl_3 \cdot 6H_2O$, 4 mmol) and 3.65 g of sodium oleate (12 mmol) has been dissolved in a mixture solvent composed of 8 mL ethanol, 6 mL distilled water and 14 mL hexane. The resulting solution has been heated to 70°C and kept at that temperature for 4 hours. At the end of the reaction, the upper organic layer containing the iron-oleate complex was washed three times with 30 mL distilled water in a separatory funnel. After washing, hexane was evaporated off, resulting in iron-tri-oleate complex in a waxy dark red solid form (2.6 g).

1.2.3. Synthesis of surfactant-coated spherical iron oxide nanoparticles (SIOs)

Spherical iron oxide nanoparticles (SIOs) synthesis has been performed by solvothermal decomposition of iron tri-oleate in octadecene refluxed at 320 °C for 1 h in the presence of oleic acid as surfactant as by Park et al [6]. Briefly, 3.6 g (4

mmol) of the iron-tri-oleate complex synthesized as described above and 5.7 g of oleic acid (20 mmol) were dissolved in 200 g of 1-octadecene at room temperature. The reaction mixture was heated to 320 °C with a constant heating rate of 3.3 °C min^{-1} and then kept at this temperature for 30 min. When the reaction temperature reached 320 °C, several reaction occurred and the initial transparent solution became turbid and brownish black. The resulting solution containing the nanocrystals was then cooled to room temperature and 50 mL of ethanol was added to the solution to precipitate the nanocrystals. The precipitate was washed several times with a mixture of hexane/acetone and the SIOs were dispersed in chloroform and stored at room temperature at a concentration of 10 mg mL^{-1}. SIOs concentration has been gained by ICP-calibration curve (in chloroform).

1.2.4. Synthesis of surfactant-coated polyhedral iron oxide nanoparticles (PIONs) with hyperthermic properties

Based on the previous synthesis we decided to synthesize polyhedral iron oxide nanoparticles (PIONs) by a slight modified solvothermal decomposition starting from the iron-oleate complex. Iron-oleate (80 mmol) was dissolved in 200 g of 1-octadecene at room temperature and 5.7 g of oleic acid (20 mmol) was added. The reaction mixture was heated to 110 °C for 1 h to remove solvent humidity, then raised to 200 °C and manteined at this temperature for additional 2 h. Next, the temperature was gradually raised (3°C/min) to reflux (320 °C) and refluxed for 2.5 h. The dark solution was finally cooled to room temperature and diluted with ethanol (100 mL) to precipitate the nanocrystals and centrifuged. The precipitate was washed several times with a mixture of hexane/acetone and the PIONs were collected and dispersed in chloroform and stored at room temperature at a concentration of 10 mg mL^{-1}. PIONs concentration has been gained by ICP-calibration curve (in chloroform).

1.2.5. Synthesis of nanocubic iron oxide nanoparticles (IONs) with hyperthermic properties

Based on a previous study [7] we decided to synthesize iron oxide nanocubes (IONs) with a diameter of 19 nm. Briefly, 0.353 g (1 mmol) of iron (III) acetylacetonate and 0.69 g (4 mmol) of decanoic acid were mixed in 25 mL of dibenzyl ether. The solution was degassed at room temperature for 45 min, then heated to 200°C (5°C/min) and kept at this temperature for 2.5 h. Finally, the temperature was increased to reflux temperature (at a rate of 10°C/min) and kept at this value for 1 h. After cooling to room temperature the IONs were collected by adding a 4-fold volume of acetone/chloroform and centrifuged at 8000 rpm. The sample was washed three times and at the end dispersed in 15 mL of chloroform.

1.2.6. Polymer synthesis for water-phase transfer

As SIOs and PIONs are hydrophobic, to transfer them in water phase we synthesized the amphiphilic polymer named PMA by condensation of poly (isobutylene-alt-maleic anhydride) with dodecylamine according to Cheng-An J. Lin [8]. To obtain a monodisperse polymer it is very important to carry out the reactions at room temperature and to use the organic solvents in anhydrous quality.

For this synthesis, as clearly described in literature [9] we placed in a round flask 3.084 g of poly-(isobutylene-alt-maleic anhydride) and dissolved 2.70 g of dodecylamine (15 mmol) in 100 mL of tetrahydrofurane.

The two solutions were vigorously mixed together, sonicated for several seconds (~20 s), and heated to 55-60 °C (just below boiling point of THF) for 1 hour. Afterwards, the solution was pre-concentrated to about one third of the original volume in a rotavap system (Laborota 4000, Heidolph) under reduced pressure (p = 200-150 mbar) in order to enhance the reaction between the polymer and the amine. Once the sample had been concentrated, it was left stirring overnight. Then, the solvent was slowly evaporated in a rotavap system until the polymer was completely dried.

Finally, the PMA was re-dissolved in 25 mL anhydrous $CHCl_3$ with a resultant concentration of 0.5 M monomers (= 12.5 mmol /25 mL).

For the functionalization of the polymer with fluoresceinamine, appropriate amounts of fluoresceinamine dissolved in EtOH (1 M) were slowly dropped into the diluted polymer solution (0.5 M) and reacted overnight under stirring. The amount of added molecules was calculated in such ways that between 0.25% and 4% of the anhydride rings of the polymer backbone were reacted. After evaporation of the organic solvent under reduced pressure, the polymer was re-dissolved in chloroform to a final concentration of 0.5 M monomers.

For IONs we used the commercial poly-(maleic anhydride alt-1-octadecene). So we dissolved this polymer in $CHCl_3$ to a final concentration of 0.5 M.

1.2.7. Water-phase transpher

SIOs, PIONs and IONs suspended in chloroform were transferred to water phase by coating them with a 0.5 M solution of the above-described polymers. The polymer solution and the nanoparticles were mixed for 30 min at room temperature (100 polymer units per nm^2 of NPs surface for SIOs and PIONs and 500 polymer units per nm^2 of NPs surface for IONs). The organic solvent was then completely evaporated under reduced pressure, and the solid is then resuspended in sodium borate buffer (SBB, 20 mM pH 12) to hydrolyze the remaining maleic anhydride groups of the polymer shell.

After this phase transfer, the nanoparticles were hydrophilic and were suspended in water by two rounds of diluition and reconcentration through an Amicon filter (50 kDa filter cutoff) (Millipore Corporation, Billerica, MA) concentrator tube by centrifuging at 3000 rpm to remove the excess unbound polymer. The resulting polymer-coated nanoparticles were dispersible and stable for at least 6 months in water phase.

Limited to the experiments with fluourescent analysis fluoresceine amine–PMA (FA@PMA) was used.

1.2.8. Particle size and surface charge analysis

Nanoparticles hydrodynamic size and surface charge were performed using a Malvern Zetasized Nano ZS ZEN3600 (Worcestershire, UK) operationg at a λ of 633 nm and a fixed scattering angle of 173°C. The sample concentration was adjusted to keep attenuator values between 7-9. The refractive index was 1.524. The measurements were performed in triplicate after dilution with MilliQ® water.

ζ-Potential measurements were elaborated on the same instrument equipped with an AQ-809 electrode soaked in 10 mM NaCl aqueous solution (pH 7.25, σ = 14.2 mS cm^{-1}), and data were processed by Zeta-Plus software. Sight distribution spectra were collected (at 23 °C) by NanoSight LM10 from NanoSight Limited (Amesbury, U.K.) and analyzed with NTA software.

1.2.9. Iron quantification by ICP analysis

The iron concentration was determined by elementary ICP-OES analysis. Briefly to 500 μL samples, were added 3 mL of aqua regia and, after 72 h, the samples were diluited with 7 mL of distilled water. All samples were measured in triplicate with Optima 700 DV ICP-OES (Perkin Elmer, Waltham, MA).

1.2.10. Hyperthermic efficiency of nanoparticles

Hyperthermic properties of nanoparticles were determined by calorimetric measures on sample exposed to the different AMF varying the frequency between 110 and 521 kHz and the magnetic field amplitude in a 9-25 mT range (Magnetherm, NanoTherics ltd, UK). Samples were placed inside an induction coil and exposed for 20 minutes to the AMF. The temperature variations were recorded with a multichannel optical fiber thermometer (Fotemp4, Optocon Systems, DE). The optical probe was placed slightly beneath the surface of the medium; a second one was placed near the induction coil and used as reference for ambient temperature. The thermal efficiency was expressed as SAR.

Because it was not possible to ensure the completely adiabatic condition of the experimental setup, this value was determined as the initial slope of the temperature increase, estimated by considering the linear term of a polynomial fitting of the heating curve of the samples [10]:

$$SAR = 1/m_e(\Sigma c_i m_i dT/dt)$$

m_e = total mass of iron
C_i = specific heat of different species in solution
m_i = weight of different species in solution
dT/dt= slope of the T(t) curve

1.2.11. Statistical Analysis

Data were expressed as mean ± standard deviation (SD). Data were analyzed by ANOVA. Post hoc analysis was carried out when statistical significance $P<0.05$ (*), and $P<0.01$ (**) was detected.

1.3. Results and Discussion

1.3.1. Synthesis and characterization of superparamagnetic iron oxide nanoparticles

Synthesizing monodisperse nanocrystals is of key importance, because the heating properties of the nanoparticles depend strongly on their shape and dimension. Here we synthesized two different kinds of monodisperse nanocrystals from organometallic precursors by solvothermal decomposition in octadecene with the aim to develop a suitable heat mediator for our study.

According to Park et al. [6] we firstly synthesized the iron-oleate complex by reacting iron chloride and sodium oleate. The iron-oleate complex was then dissolved in 1-octadecene and slowly heated to 320° aging at that temperature for 30 min (Figure 1).

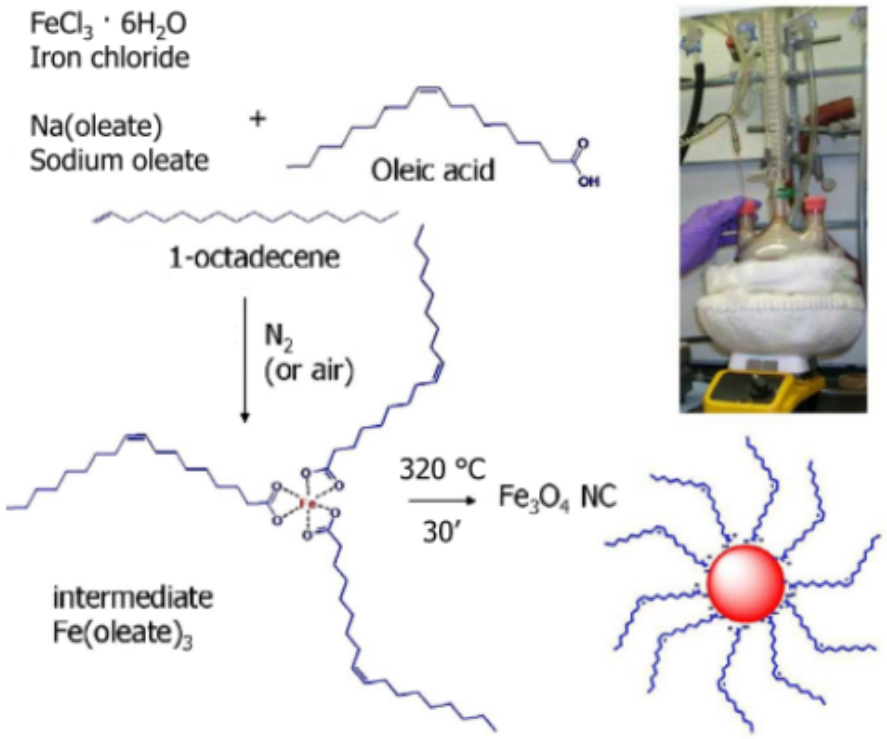

Figure 1: synthesis of iron oxide nanocrystals [6].

"The iron-oleate complex acts as the growth source for the synthesis. Nucleation occurs at 200-240 °C triggered by the dissociation of one oleate ligand from $Fe(oleate)_3$ precursor by CO_2 elimination. The major growth occurs at 300°C

iniziated by the dissociation of the remaining two oleate ligands from the iron-oleate species" [6]. The high temperature and the presence of stabilizing surfactants provided an optimal crystal nucleation and growth resulting in highly uniform and monodisperse nanoparticles.

Moreover, as clearly described by Park et al. the choice of the solvent is highly relevant for the particle size, which depends on the boiling point of the solvent. We chose 1-octadecene (b.p. 317°C) to obtain highly uniform and monodisperse spherical nanocrystals (SIOs).

Unfortunately, as these nanoparticles did not shown hyperthermic properties, we decided to modify the procedure to obtain larger nanoparticles usable for hyperthermia. These nanoparticles were prepared by first keeping the iron tri-oleate solution in oleic acid/octadecene at 200 °C for 2 h, then gradually raising the temperature (3 °C/min) to reflux, refluxing for 2.5 h and finally cooling the dark solution to room temperature. In this way, we obtained polyhedral iron oxide nanocrystals (PIOs) with high SAR values.

1.3.2. Polymer Synthesis

An amphiphilic polymer was synthesized as coating agent according to the inventor Chen-An J. Lin in order to obtain water-soluble sPIONs [8]. The polymer is based on a poly-(maleic anhydride) backbone. This backbone represents the hydrophilic part, instead the hydrophobic side chains are constructed by a reaction of the anhydride rings with the amino-groups of dodecylamine. The concept of this polymer has been successfully demonstrated in several work of Parak's group [9,11]. The maleic anhydride groups of the PMA backbone have been assumed to be 100 % reactive to primary amino-ligands through spontaneous amide linkage, which converts one maleic anhydride group into one corresponding amide and one free carboxylic acid group.

It's important to underline that we chose to react only the 75% of the anhydride rings with the amino-group of dodecylamine. The remaining 25 % of the anhydride rings were used in a second step for linking additional functional molecules. For instance, we conjugated 1% of the remaining anhydride rings with fluoresceinamine as organic fluorophore for the required fluorescence assays. In this way the

alkylamines of the fluoresceinamine can directly linked to the anhydride rings by the reaction of the anhydride with the amine.

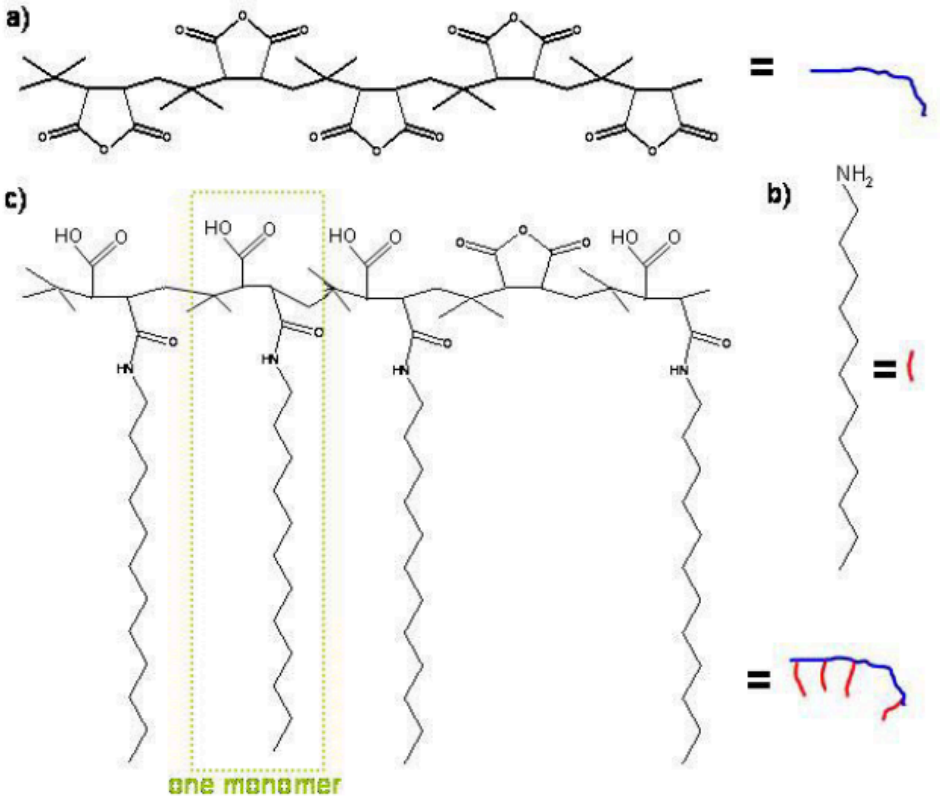

Figure 2: Chemical structure of the polymer. a) poly-(isobutylene-alt-maleic anhydride) backbone (hydrophilic part). b) dodecylamine (hydrophobic part) C) conjugation of the polymer with the dodecylamine. Each monomer unit comprises one anhydride ring. At the end we obtained an amphiphilic polymer with and hydrophilic backbone and a hydrophobic sidechain [9].

1.3.3. Water-phase transfer

Because of their biological application, colloidal stability and water phase transfer of magnetic iron oxide nanoparticles are required. Thus, SPIONs were coated with the above-described PMA. In the coating process, the hydrophobic alkyl chains intercalated between those of oleic acid, which acted as surfactant, instead the hydrophilic backbone lend to the water solubility of the nanoparticle. So, the PMA is wrapped around the nanoparticles and the organic solvent is replaced by acqueous solution enabling the phase transfer to aqueos solution.

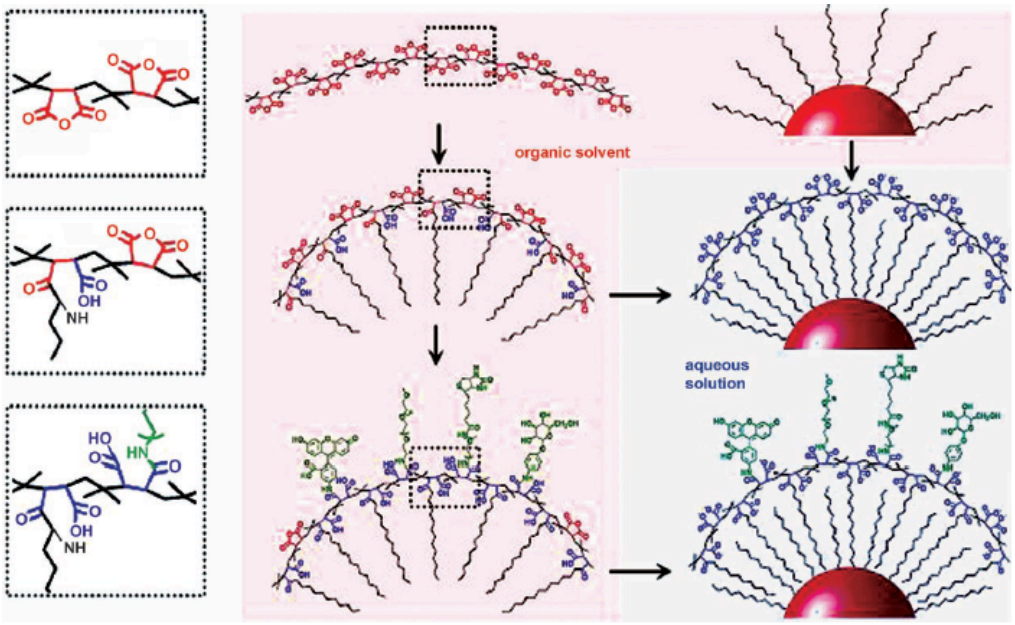

Figure 3: Scheme of the polymer coating procedure [8].

Upon phase transfer to water solution the remaining maleic anhydride groups of the polymer were hydrolyzed with Sodium Borate Buffer at pH 12 and then the nanoparticles were transferred to water phase to yield negatively charged carboxyl groups, which provide electrostatic repulsion lending to stable dispersion of nanoparticles.

Phase transfer resulted in three different hydrophilic nanoparticle aqueos solutions: spherical shape iron oxide nanoparticles (SIOs) as determined by Transmission Electron Microscopy (TEM) (Figure 4A) with a diameter of 12.6 ± 0.4 nm as measured by dynamic light scattering (DLS) (Figure 4B) and with a ζ-potential of –59.3 ± 2.3 mV (Figure 4C), likely suggesting a high stability of SIOs with minimum aggregation at physiological pH. In fact, a zeta potential value higher than ± 30 mV is generally required for a colloidally stable nanoparticle dispersion [12].

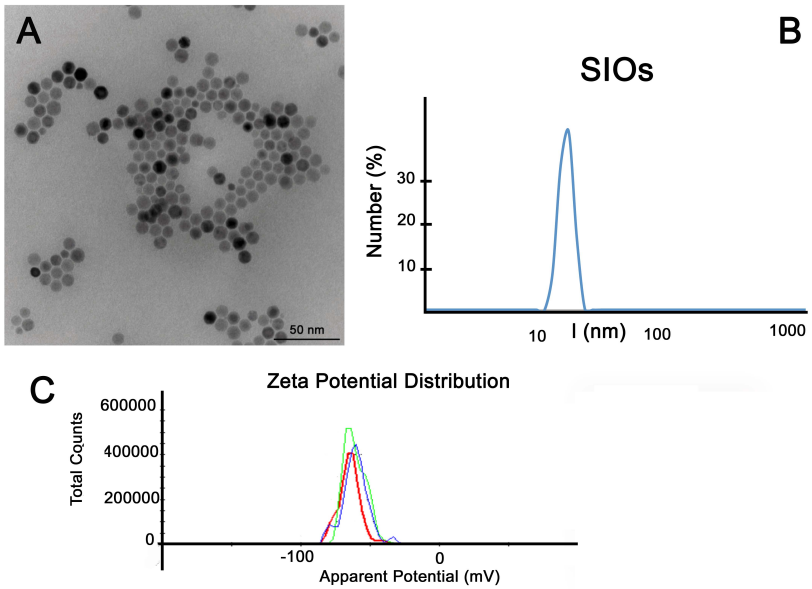

Figure 4: Physical characterization of SIOs. A) Transmission electron microscopy image of SIOs. B) Size distribution of SIOs by DLS measure. C) Zeta Pontential Distribution of SIOs by Zeta-Sizer Analysis.

We also obtained polyhedral iron oxide nanoparticles (PIONs) consisting of a mixture of nanocubes, truncated octahedral and irregular polyhedral as determined by TEM (Figure 5A) with batch-to-batch reproducibility, having an average size of 25.1 ± 0.1 nm as detemined by DLS (Figure 5B) and a ζ–potential of –68.9 ± 4.3 mV (Figure 5C). Also in this case, the zeta potential suggests a high stability in a physiological milieu.

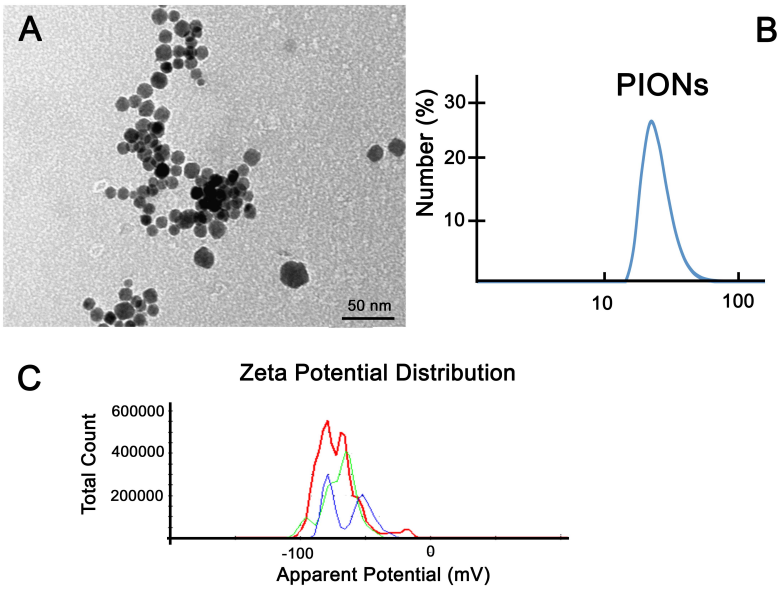

Figure 2: Physical characterization of PIONs. A) Transmission electron microscopy image of PIONs. B) Size distribution of PIONs by DLS measure. C) Zeta Potential Distribution of PIONs by Zeta Potential Analysis.

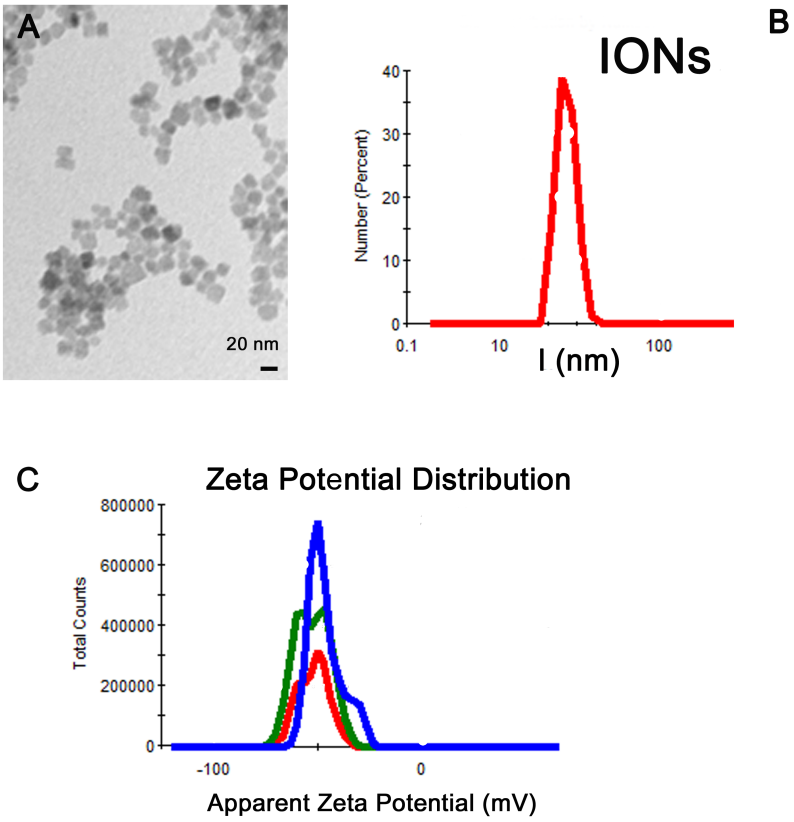

Figura 6: Physical characterization of IONs. A) Transmission electron microscopy of IONs. B) Size distribution of IONs by DLS measure. C) Zeta Potential Distribution of IONs by Zeta Potential Analysis.

Alternatively we obtained cubic iron oxide as determined by Transmission Electron Microscopy (TEM) (Figure 6A) with a diameter of 19.6 ± 0.4 nm as measured by dynamic light scattering (DLS) (Figure 6B) and with a ζ-potential of –69.3 ± 2.3 mV (Figure 6C), likely suggesting a high stability of IONs with minimum aggregation at physiological pH.

1.3.4. Determination of the hyperthermic power of SPIONs in acqueos medium

We assessed the magnetic hyperthermia (MHT) efficiency of SPIONs in aqueous suspension at a [Fe] of 4 mM (corresponding to ~1 mg mL^{-1}) by varying the frequencies between 110 and 521 kHz and the magnetic field amplitude in a 9-25 mT range. While the hyperthermic efficiency of SIOs was negligible at all tested frequencies, PIONs exhibited frequency-dependent heat capacity with an optimal response at 521 KHz and 25 mT (Figure 6 A-B). Because the measurements were performed in non-adiabatic conditions, the curve slopes were fitted only in the first 30 s. SAR values relative to the different conditions are summarized in Figure 6B.

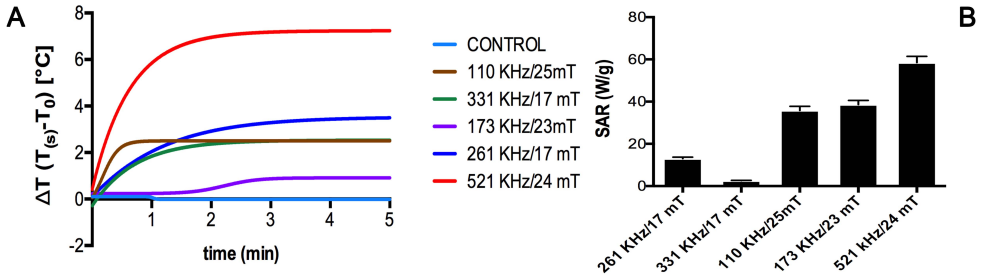

Figure 6: A) Temperature variation as a function of AMF exposure time measured on a sample of PIOs containing iron at a concentration of 4 mM. B) SAR values as a function of AMF exposure.

Then we tested the MHT by varying the concentration between 3 and 25 mM (Fig. 7, A and B). The amount of heat produced by SMHT increased linearly with PION concentration (Fig. 7, A and B). The application of MHT to the sample resulted in a temperature increase of 20 °C after 120 s reaching a plateau after 6 minutes with a maximal ΔT of 22.5 °C.

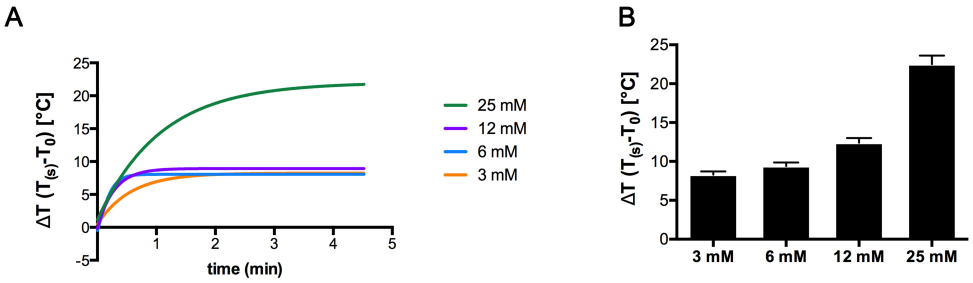

Figure 7: A) temperature variation as a function of iron concentration on a sample of PIOs exposed to an AMF of 521 KHz and 24 mT. B) histogram representation of the temperature variation.

Therefore, our results suggested that only PIONs could provide heat capacity suitable for utilization as hyperthermic mediators and PIONs were thus selected for the biological study. Physical charatecterization and best heating curve of PIONs were summarized in Figure 8.

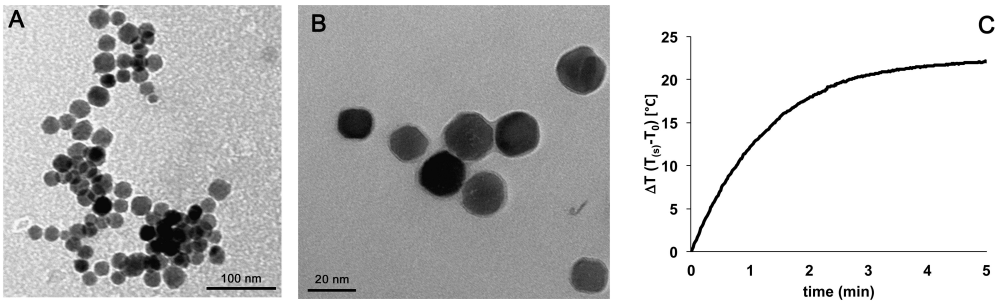

Figure 3: Physical characterization of PIONs. A,B) Transmisson electron microscopy images of PIONs at different scaling. C) Temperature variation of AMF exposure time measured on a sample of PIONs containig iron at a concentration of 25 mM (MHT at 521 KHz, 25 mT).

Unfortunately the hyperthermic efficiency of IONs was negligible at all tested frequencies. This result suggests us to optimize the synthesis procedure.

1.4. Conclusions

As reported in literature, not every kind of SPIONs is able to induce heat. Thus, slighty modifying a well-known synthetic procedure, we developed a new efficient nanoparticles responsive to AMF and usable for SMHT. This approach is expected to be of general utility and may become a universal strategy for the development of new efficient nanoparticles for thermotherapy.

My results suggested that only PIONs were able to induce heat when subjected to an AMF and only them could provide heat capacity sufficiently suitable for the utilization as heating mediators in our *in vitro* model for adipocyte cells. Thus, for the first application we decided to use PIONs as heating mediators in adipocytes causing an impact on the adipocytes triglyceride metabolism.

For the second study we decided to develop a nanoparticle with a better heating capacity, as we wanted to induce death in tumour cells. Thus, as the heating capacity strongly depends on the shape of the magnetic nanoparticles we decided to synthesize iron oxide nanocubes (IONs) as the best heating mediators for hyperthermia on glioblastoma.

Unfortunately the hyperthermic efficiency of IONs was negligible at all tested frequencies. This result suggests us to spend more time trying to optimize the synthesis procedure obtaining better heating mediator.

1.5. References

[1] Gilchrist, R. K., et al., Selective inductive heating of lymph nodes. *Ann Surg.* 146 (1957) 596-606.

[2] Hergt, R., et al., Magnetic Particle Hyperthermia: Nanoparticle Magnetism and Materials Development for Cancer Therapy. *J. Phys.: Condens. Matter* 18 (2006) S2919-S2934.

[3] Rosensweig, R. E., Heating Magnetic Fluid with Alternating Magnetic Field. *J. Magn. Magn. Mater* 252 (2002) 370-374.

[4] De la Presa, P., et al., Study of Heating Efficiency as a Function of Concentration, Size, and Applied Field in γ- Fe2O3 Nanoparticles. *J.Phys.Chem. C* 116 (2012) 25602-25610.

[5] Dutz, S., et al., Magnetic nanoparticle heating and heat transfer on a microscale: Basic principles, realities and physical limitations of hyperthermia for tumour therapy. *Int. J. Hyperthermia* 29 (2013) 790-800.

[6] Park, J., et al., Ultra-large-scale syntheses of monodisperse nanocrystals. *Nat. Mater.* 3 (2004) 891–895.

[7] Guardia, P., et al., Water-soluble iron oxide nanocubes with high values of specific absorption rate for cancer cell hyperthermia treatment. *ACS Nano* 6 (2012) 3080–3091.

[8] Lin, C. A. J., et al., Design of an amphiphilic polymer for nanoparticle coating and functionalization. *Small* 4 (2008) 334–341.

[9] Fernández-Argüelles, M. T., et al., Synthesis and Characterization of Polymer-Coated Quantum Dots with Integrated Acceptor Dyes as FRET-Based Nanoprobes. *Nanolett.* 7 (2007) 2613-2617.

[10] Lartigue, L., et al., Water-dispersable sugar-coated iron oxide nanoparticles. An evaluation of their relaxometric and hyperthermia properties. *J. Am. Chem. Soc.* 133 (2011) 10459-10472.

[11] Pellegrino, T., et al., Hydrophobic Nanocrystals Coated with an Amphiphilic Polymer Shell: A General Route to Water Soluble Nanocrystals. *Nanolett.* 4 (2004) 703-707.

[12] Bazylinska, U., et al., Dicephalic ionic surfactants in fabrication of biocompatible nanoemulsions: factors influencing droplet size and stability. *Colloids Surf. A. Physicochem. Eng. Asp.* 460 (2014) 312-320.

Chapter 2

Application of Thermotherapy to adipose tissue

2.1 Introduction

2.1.1. Adipose Tissue Reduction

The involvement of overweight and obesity on the pathogenesis and aggravation of several life-threatening diseases, including diabetes mellitus, cancer, cardiac and liver diseases, and of fatal events, such as stroke and myocardial infarction, is now well established. So there is an urgent need to develop new efficient treatments for the adipose tissue reduction.

At present, the reduction of adipose tissue is obtained by different invasive and non-invasive techniques, including bariatric surgery, liposuction, laser, ultrasounds, cryolipolysis, and radiofrequency, which however do not change the energy balance equation and are subjected to detrimental side effects. Moreover in some cases these treatments require electronic devices raising the temperature in all the tissues exposed to heating source without any selective effect on the adipose tissue [1-3].

Also some pharmacological agents, including sibutramine rimonabant, are now withdrawn from the market, and others like amphetamine and orlistat are used in the management of obesity [4]. They operate like anorexizant agents on the appetite suppression interacting with central receptors or on the suppression of fat absorption by the first tract of gut. However these drugs showed limited efficacy and unacceptable side effects (strokes, intestinal serious side effect, kidney failure, severe hepatotoxicity or correlation with a higher incidence of cancer), leading to the withdrawn from the market or strict limitations on their use [5].

However little is known about the biomechanism of obesity and overweight in humans. These patologies result in a dysregulation in circulating hormones that affect systemic energy balance leading to several life-threating diseases, including type 2 diabetes mellitus (T2D), stroke, heart and liver disease, and enhancing the cancer risk [6-11].

Thus, understanding the molecular and cellular events regulating the mechanisms of hyperplasia and hypertrophy in adipose tissue is crucial to design rational therapies to prevent and treat obesity avoiding side effects [12].

Adipose tissue grows by two mechanisms: hyperplasia (cell number increase) and hypertrophy (cell size increase) [13]. The hyperplasia and the hypertrophy in

adipocytes are determined by a metabolic imbalance between the triglyceride storage and removal referred as lipolysis. This catabolic process is precisely regulated through hormonal and biochemical signals that concur to the rapid turnover of lipids within the fat cells [14]. Lipolysis is a key of importance for the turnover of lipids in the fat cells; indeed a dysregulation of this turnover underlines several pathological conditions. The "canonical pathway" takes place in the lipid droplets with other co-working enzymes involved in the regulation of metabolic processes [15, 16]. "Canonical lipolysis" is tightly regulated via adipose triglyceride lipase (ATGL), the limiting-step enzyme in the triglyceride metabolism, producing diacylglycerol, metabolized by a hormone-sensitive lipase (HSL) into glycerol and fatty acids.

2.1.2. Aim of the work

Several studies proved that heat shock produces alteration in energy metabolism of white adipose tissue resulting in the liberation of glycerol and fatty acids used by other organs as energy substrates [17].

Even if the use of iron oxide nanoparticles as heat mediators is mainly dedicated to cancer thermotherapy, we reasoned that our Polyhedral Iron Oxide nanoparticles (PIONs) presented in Chapter 1 could be also exploited to induce a monitored hyperthermic effect in white adipocytes without any cellular damage or toxic effect.

As our PIONs exhibited effective heat capacity in aqueos solution when subjected to an alternating magnetic field (AMF), the aim of the present study was to investigate the effect of applying intracellular superparamagnetic hyperthermic treatment (SMHT) in reducing the lipid content in mature adipocytes as a novel strategy to counteract obesity and the multiple pathologies associated.

2.2. Materials and Methods

2.2.1. Cell cultures

3T3-L1 preadipocytes (ECACC, Sigma-Aldrich, St. Louis, MO, USA) were sub cultured in Dulbecco's modified Eagle's medium nutrient mixture F12 (DMEM-F12) containing 10% fetal bovine serum, 100 units mL^{-1} penicillin and 100 μg mL^{-1} streptomycin in a humidified incubator at 37 °C with 5% CO_2. To stimulate differentiation into adipocytes the cells were grown to confluency in 35x10 mm Petri dish and then were differentiated in accordance with a well-established standard adipocyte differentiation kit (3T3-L1 Differentiation Kit, Sigma-Aldrich, St. Louis, MO, USA). After 3-days of induction the medium was changed and the cells were matured in high-glucose Dulbecco's modified Eagle's medium containing 10 μg mL^{-1} of insulin. Eight-days post-induction cells were subjected to the different treatments.

2.2.2. Cell viability Assay

The cytotoxicity of PIONs toward adipocytes was assessed by the loss of cells viability using 3-(4,5-dimethylthiazol-2-yl)-2,5-diphenyltetrazolium bromide) (MTT) test. Adipocytes were seeded (5×10^3 cells per well) in a 96-well plate and grown for 24 h in a humidified incubator at 37 °C with 5% CO_2. After 24 h the medium was replaced with fresh medium containing different PIONs concentrations (10, 20, 50 100 μg mL^{-1}). After 6, 12, 24, 48 h of exposure at 37 °C, cells were washed with PBS 1X and then incubated for 3 h at 37 °C with 0.1 mL of 3-(4,5-dimethyl-2-thiazolyl)-2,5-diphenyl-2H-tetrazolium bromide (MTT) stock solution previously diluted 1:10 in DMEM-F12 medium without phenol red. After incubation, dimethyl sulfoxide (0.1 mL) was added to each well to solubilize the formazan. The absorbance in each well was read by a microplate reader (CHROMATE 4300 Awareness Technology, USA) at a wavelength of 570 nm using a reference wavelength of 620 nm.

The test was conducted in triplicate. Statistical comparisons between treated and control samples were performed by using the non-parametric Mann Whitney U test. The cell viability (%) was calculated with the following equation:

$$CV\% = \left(\frac{OD_{sample}}{OD_{control}}\right) \times 100$$

2.2.3. Flow cytometry analysis of PIONs internalization

8-Days post-induction adipocytes were incubated with 10, 20 and 50 μg mL^{-1} of fluoresceinamine@PIONs (FA@PIONs) at different time-points (15 min, 4, 24, 48 h) at 37 °C with 5% CO_2. After treatments, cells were washed with PBS 1X, detached and analyzed by flow cytometry in order to quantify the percentage of positive cell population. Sample acquisition (10000 events) was performed by Gallios Flow cytometer (Beckman Coulter Inc.) and analyzed by FlowJo Software. The analysis was conducted in triplicate and statistical analysis was performed by using the one-way Anova test.

2.2.4. Confocal Laser Scanning Microscopy

For Confocal Laser Scanning Microscopy, 8-days post-induction adipocytes were incubated with three different concentrations of FA@PIONs (10, 20, 50 μg mL^{-1}) at four different time-points (15 min, 4, 24, 48 h). The culture medium was then removed by aspiration from the coverslips and gently washed with PBS at room temperature. The cells were then fixed with 4% buffered formalin for 30 min at room temperature. The coverslips were washed out of the formalin with PBS for 2 minutes. For the permeabilization the coverslips were incubated in 0.5% Triton X-100 with PBS for 5 min. The typically adipocyte overexpression of the Glucose Transporter GLUT4 was marked with Antibody NBP1-49533AF647 (Novus Biologicals Europe, UK) labeled with AlexaFluor®647. The antibody was firstly diluited in BSA to a final concentration of 14 μg/mL and then the coverslips were incubated with the antibody for 1 h at room temperature in a dark environment. The coverslips were washed gently in PBS for three times 5 minutes each. The nuclei were then stained with HOECHST 3342 diluited in PBS to a final concentration of 0.2 mM. The coverslips were then inverted onto a glass slip with a

drop of Entellan® as mounting media. Images were obtained with Leica TCS SP5 inverted confocal microscope (Leica). DM IRE2 confocal microscope equipped with an argon/krypton laser. Three laser lines were activated UV (405 nm), Visible (488 nm) and Visible (633 nm). A 40x objective (oil immersed, numerical aperture 1) was used. To acquire and merge the images the Leica LAS AF software (Leica) was employed. Image contrast in each channel was then set using ImageJ software. At least 5 fields per each sample of two biological replicates were taken.

2.2.5. SMHT treatment

Based on the results of cell viability and the internalization test, 3T3-L1 adipocytes were incubated for 24 h with 50 μg mL^{-1} of PIONs into a Petri dish. After 24 h the treated cells were placed inside the coil and exposed for 20 minutes to an AMF with a frequency of 521 KHz and strength of 25 mT. The cells were processed for the triglyceride quantification, glycerol content in the medium, ultrastructural morphology and qRT-PCR immediately after SMHT and 24 h post-hyperthermia.

Statistical comparisons between treated and control samples were performed by using the Mann Whitney U test.

2.2.6. qRT-PCR

Total RNA was isolated from the control and treated adipocytes using RNA-easy Plus Mini Kit (QIAGEN; Milan, Italy). RNA (1.5 mg) was reverse transcribed using High Capacity cDNA Reverse Transcription Kit (Applied Biosystems; Monza, Italy) and amplified using a StepOnePlus Real-Time PCR System (Applied Biosystems; Monza, Italy). The target cDNAs were amplified using SYBR® Green PCR Master Mix (Invitrogen; Monza, Italy) together with gene-specific primers for *peroxisome proliferator-activated receptor γ, PPARγ* (fwd: AGAGATGTGCAAACAGGGCT, rev: GCAAAGGGTTGGGTTGGTTC); *adipsin* (fwd: *GTGCAGAGTGTAGTGCCTCA, rev: CCAACGAGGCATTCTGGGAT); adiponectin* (fwd: ATCTGGAGGTGGGAGACCAA; rev: GGGCTATGGGTAGTTGCAGT); *adipose triglyceride lipase, ATGL (*fwd: AGAGATGTGCAAACAGGGCT, rev: GCAAAGGGTTGGGTTGGTTC); *p53* (fwd: AAACGCTTCGAGATGTTCCG; rev: CTTCAGGTAGCTGGAGTGAGC); *b-actin* (fwd:

CATCGTGGGCCGCTCTA, rev: CACCCACATAGGAGTCCTTCTG). PCR conditions were 95 °C for 20 s, 95 °C for 3 s, and 60 °C for 30 s for 40 cycles. PCR products were measured using a StepOnePlus Real-time PCR System (Applied Biosystems; Monza, Italy) and relative ratios were calculated using the $2^{(-\Delta\Delta C_T)}$ method [18]. Data were expressed as fold changes to control. Statistical comparisons were performed by using the Mann Whitney U test.

2.2.7. Transmission Electron Microscopy

For transmission electron microscopy, the cells were fixed with 2.5% (v/v) glutaraldehyde and 2% (v/v) paraformaldehyde in 0.1 M phosphate buffer, pH 7.4, at 4° C for 1 h, post-fixed with 1% osmium tetroxide and 1.5% potassium ferrocyanide at room temperature for 1 h, dehydrated with acetone and embedded in Epon. Ultrathin sections were stained with lead citrate and observed in a Philips Morgagni transmission electron microscope (FEI Company Italia Srl, Milan, Italy) operating at 80 kV and equipped with a Megaview II camera for digital image acquisition.

2.2.8. Oil Red O staining and intracellular triglyceride quantification

The degree of adipocyte differentiation and lipid accumulation of cytoplasmic triglycerides were detected by staining with Oil Red O (Bio-Optica, Milan, Italy). Briefly, the cells were washed in PBS, fixed with 4% buffered formalin for 30 min at room temperature. Once formalin was discarded, cells were stained for 20 min with 0.5 % Oil Red O solution. The nuclei were stained for 2 min with hematoxylin. The stained cells were photographed at 10×, 20× and 40× optical magnification using an Olympus microscope (BX-URA2, Olympus optical, GMBH, Hamburg, Germany) equipped with Image ProPlus software (Media Cybernetics, Rockville, USA). The triglyceride quantification was determined by measuring the lipid droplets content. Stained droplets were dissolved in isopropanol and then quantified by measuring absorbance at 490 nm with a VICTORTM X Series Multilabel Plate Reader. The results are shown as relative triglyceride content compared with the control according to Ramírez-Zacarías et al. [19]. Statistical analysis was conducted by using the Mann Whitney U test.

2.2.9. Glycerol analysis of release of fatty acid from adipocytes exposed to SMHT

The lipolytic effect of PIONs in 3T3-L1 adipocytes was determined by measuring the amount of glycerol released into the medium after hyperthermia treatment. Glycerol concentration was measured using a Glycerol Assay Kit (Sigma-Aldrich, St. Louis, MO, USA). In this kit, glycerol concentration is determined by a coupled enzyme assay involving glycerol kinase and glycerol phosphate oxidase, resulting in a colorimetric product (λ_{max}= 570 nm). The concentration of glycerol in the samples has been determined from the standard curve using the equation:

$$C = \frac{A_{570\ sample}}{slope}$$

C = concentration of glycerol in sample (mM);

slope = slope determined from standard curve.

The test was conducted in triplicate and statistical comparisons were performed by using the Mann Whitney U test.

2.3. Results and Discussion

2.3.1. PIONs toxicity in 3T3-L1 adipocyte cells

To test the impact of the different PIONs concentrations on cellular viability 3T3-L1 adipocytes were incubated with 10, 20, 50 and 100 μg mL^{1} of PIONs in DMEM-F12 with 10 μg mL^{-1} of insulin at 37 °C for 6, 12, 24 and 48 h. MTT Assay monitored the extent of cellular viability. Figure 1 shows the time- and dose-dependent decrease in cell viability. Only samples treated with 100 μg mL^{-1} nanoparticles exhibited percentage of cell viability fraction lower than 80% at 6 h, reaching a minimum between 24 and 48 h. Therefore MTT assay suggested that PIONs were safe up to the concentration of 50 μg mL^{-1} at short and long incubation time, whereas 100 μg mL^{-1} PIONs induced a significant increase in cell death already after 6 h incubation.

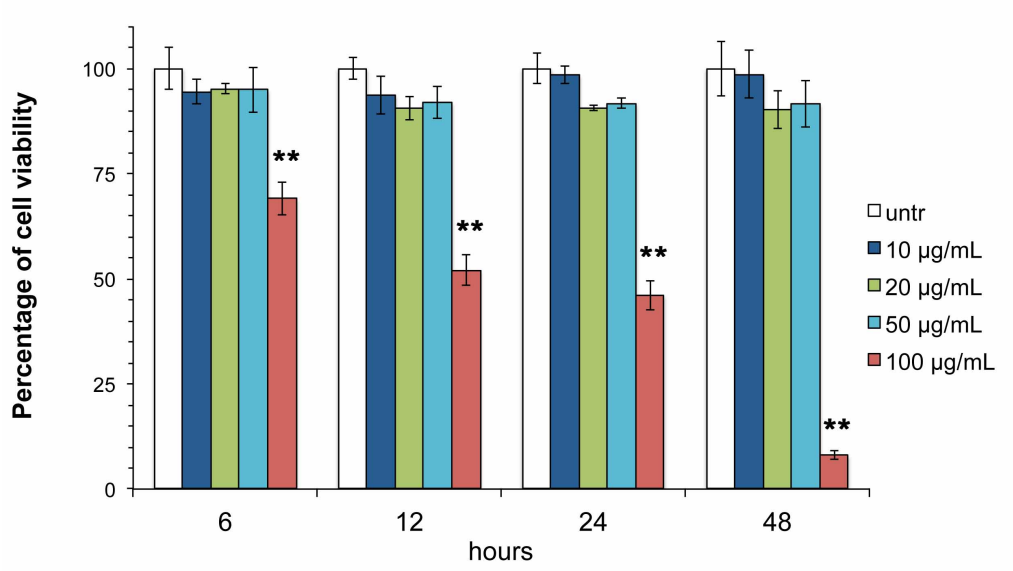

Figure 1: MTT Assay at 6, 12, 24, 48 h after PIONs uptake. **P< 0.001 *vs.* untreated.

2.3.2. PIONs uptake in 3T3-L1 adipocyte cells

For the following experiments only PIONs concentrations safe for adipocytes were used. Eight days post-induction, mature adipocytes were incubated with 10, 20 and 50 μg mL^{1} of dye-labeled PIONs with fluoresceinamine (FA@PIONs) in DMEM-F12 with 10 μg mL^{-1} of insulin at 37 °C for 15 min, 4, 24 and 48 h. Figure

2 shows time- and dose-dependent increase in uptake. Only samples treated with 50 μg mL^{-1} nanoparticles exhibited labeling fraction higher than 20% at 4 h, reaching maximal cell labeling between 24 and 48 h.

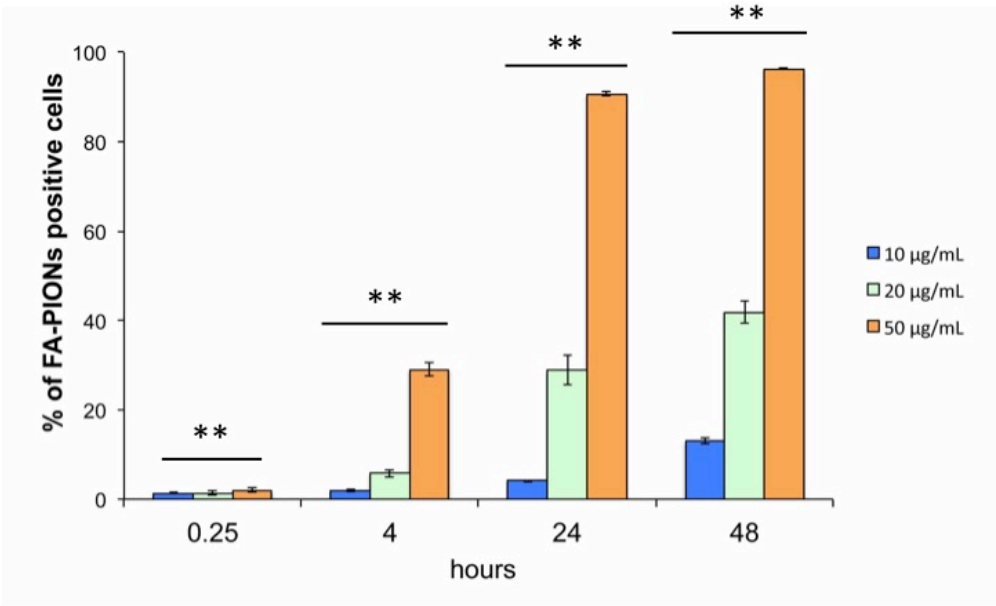

Figure 2: PIONs uptake in 3T3-L1 adipocytes. Flow cytometry analysis of FA-PIONs internalized by adipocytes represented as percentage of FA-positive cells compared to untreated cells. Histograms show a dose- and time-dependent uptake. **P < 0.01 *vs.* untreated.

In order to confirm the internalization of PIONs in 3T3-L1-derived adipocytes, cells labelled for GLUT4 were incubated for 24 h at 37 °C with 10, 20, 50 mg mL^{-1} of FA@PIONs, and analyzed by confocal microscopy (Figure 3). Images show a dose-dependent PIONs uptake, with a maximal internalization at the concentration of 50 μg mL^{-1}.

Interestingly, most of the internalized green fluorescent FA@PIONs appear as yellow dots due to the overlapping with the red signal of the membrane receptor Glut4, thus suggesting an endocytotic processes. Moreover, 50 μg mL^{-1} of PIONs did not change the expression of GLUT4 receptor, a key marker of 3T3-L1 adipocyte differentiation, indicating that PIONs uptake did not interfere with the differentiation process. Moreover, confocal microscopy also reveals the safety of PIONs because of, once internalized, PIONs still remained confined in the

cytoplasm, never entering the nucleus even at the longest incubation time. Entering the nucleus may represent a risk for the cell function, because of the possible interaction between PIONs and nucleic acid.

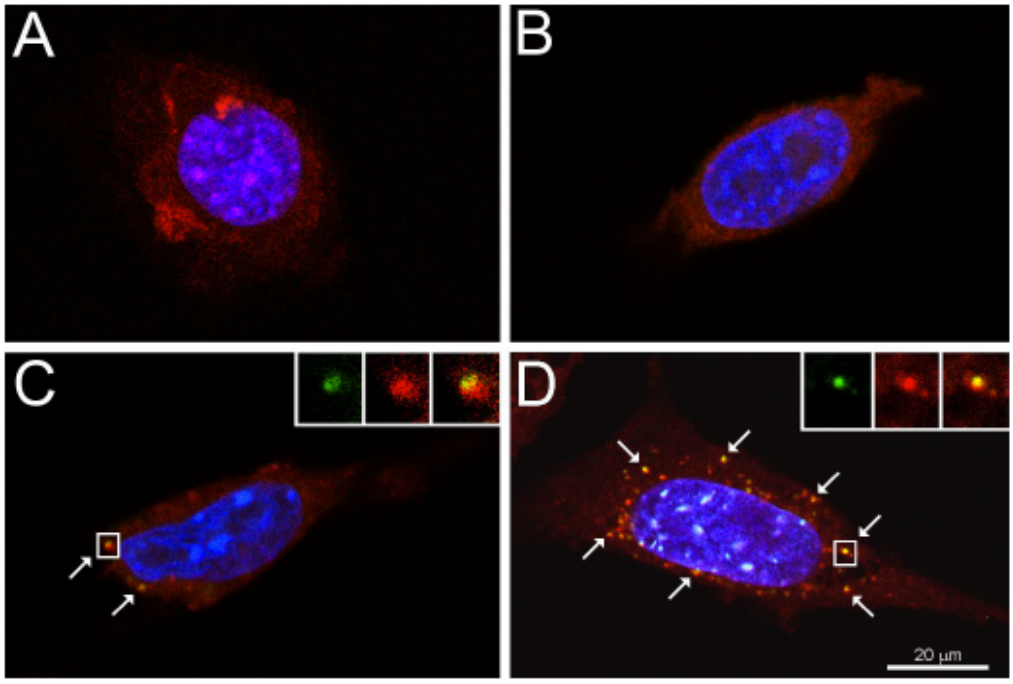

Figure 3: Intracellular localization of PIONs. Confocal microscopy merged images of 3T3-L1 adipocytes after 24 h incubation with A) 0 mg mL^{-1} (control), B) 10 µg mL^{-1}, C) 20 µg mL^{-1}, and D) 50 µg mL^{-1} FA-PIONs (green). Cell membrane receptors were detected with the anti-Glut4 antibody (red) and nuclei were stained with Hoechst (blue). Arrows indicate internalized FA-PIONs (their green signal ovelaps the Glut4 red signal thus appearing as yellow dots). Note the evident staining of Glut4 (overexpressed in adipocytes) in all samples, demonstrating that treatment does not induce dedifferentiation.

These data were corroborated by TEM analysis (Figure 4) of adipocytes treated with 50 µg mL^{-1} PIONs at 37 °C. Ultrastructural observations demonstrated that PIONs were internalized *via* endocytosis and enclosed in endosomes (Figure 4, A and B): once in the cytoplasm, the PIONs were always compartmentalized into both endosomes (Figure 4C) and residual bodies (Figure 4D), often occurring very close to lipid droplets (Figure 4E). No structural cell damage was observed following PIONs internalization.

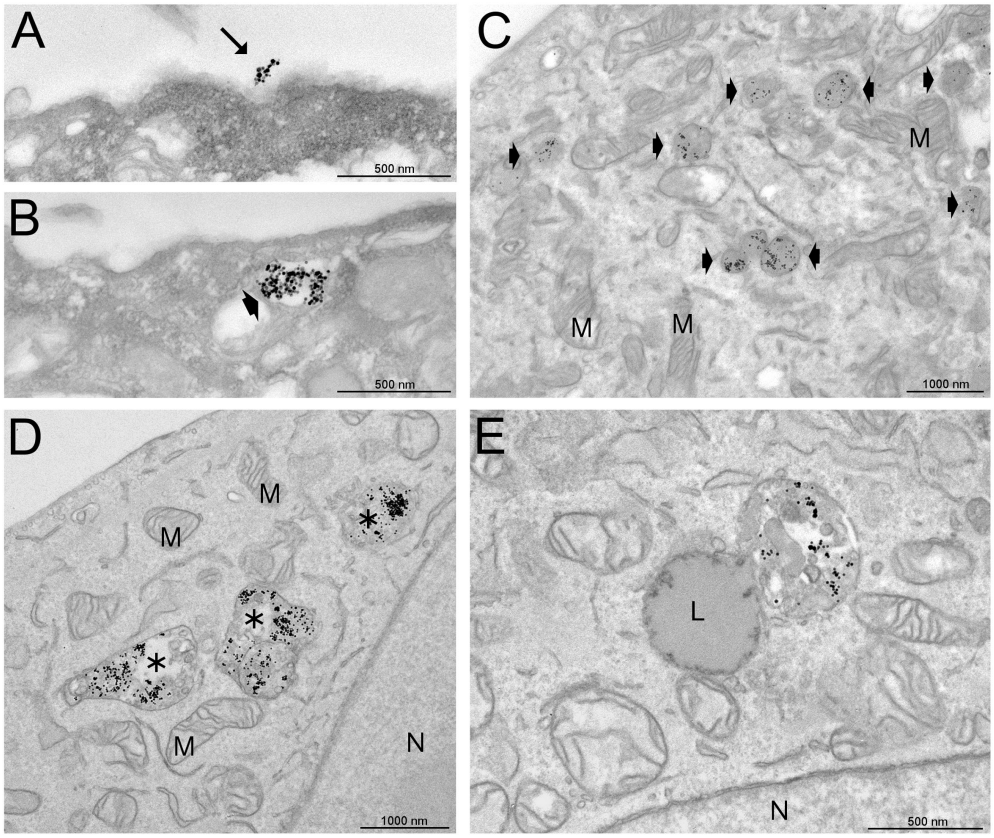

Figure 4: TEM images of PIONs uptake and intracellular distribution in 3T3-L1 adipocytes after 24 h incubation with PIONs (50 µg mL^{-1}). A) PIONs were internalized by adipocytes *via* endocytosis (arrow) and B) compartmentalized into endosomes (arrowhead). C) PIONs accumulated inside many endosomes (arrowheads) ubiquitously distributed in the cytoplasm, D) as well as in residual bodies (asterisks) also containing heterogeneous cell remnants. Mitochondria (M) and endoplasmic reticulum cisternae were abundant and well structured, demonstrating the absence of cell damage. E) Residual bodies containing PIONs also occurred very close to lipid droplets (L). N: cell nucleus.

2.3.3. Impact of SMHT on intracellular distribution and cytotoxicity of PIONs in adipocytes

Based on the previous results we chose to induce the SMHT treating 3T3-L1 adipocytes 24 h with 50 μg mL^{-1} of PIONs incubation. The adipocytes were positioned in an induction coil and subjected to an AMF for 20 min (MHT at 521 KHz, 25 mT).

Ultrastructural analysis showed no ultrastructural cell damage immediately after and 24 h after SMHT (Figure 5). TEM images showed interruptions in the membranes of the residual bodies caused by the entrapped PIONs. This broken event allows their release into the cytoplasm (Figure 5A) and their accumulation around and even into the lipid droplets (Figure 5B). Some lipid droplets were also extruded from the cell suggesting a lipolytic effect (Figure 5C).

Large amounts of PIONs were found into adipocytes until 48 h, suggesting a long-lasting cytoplasmic persistence. 24 h after SMHT were found only few and small lipid droplets in the cytoplasm. No ultrastructural cell damage was observed following PIONs internalization until 48 h incubation, confirming the safety of these nanoparticles at the concentration used (Figure 5D).

A further advantage is that PIONs occurring in the cytoplasm are often enclosed in vesicular structures, *i.e.*, endosomes formed during the endocytic process and residual bodies derived from the lytic pathways. These are important data, because a cell damage could prelude to necrotic or apoptotic processes responsible for inflammatory events *in vivo*. Moreover, since PIONs were still confined in the endosomes even after long incubation times the iron contained in PIONs never get in contact with the cytosol avoiding a potential source of oxidative stress [20].

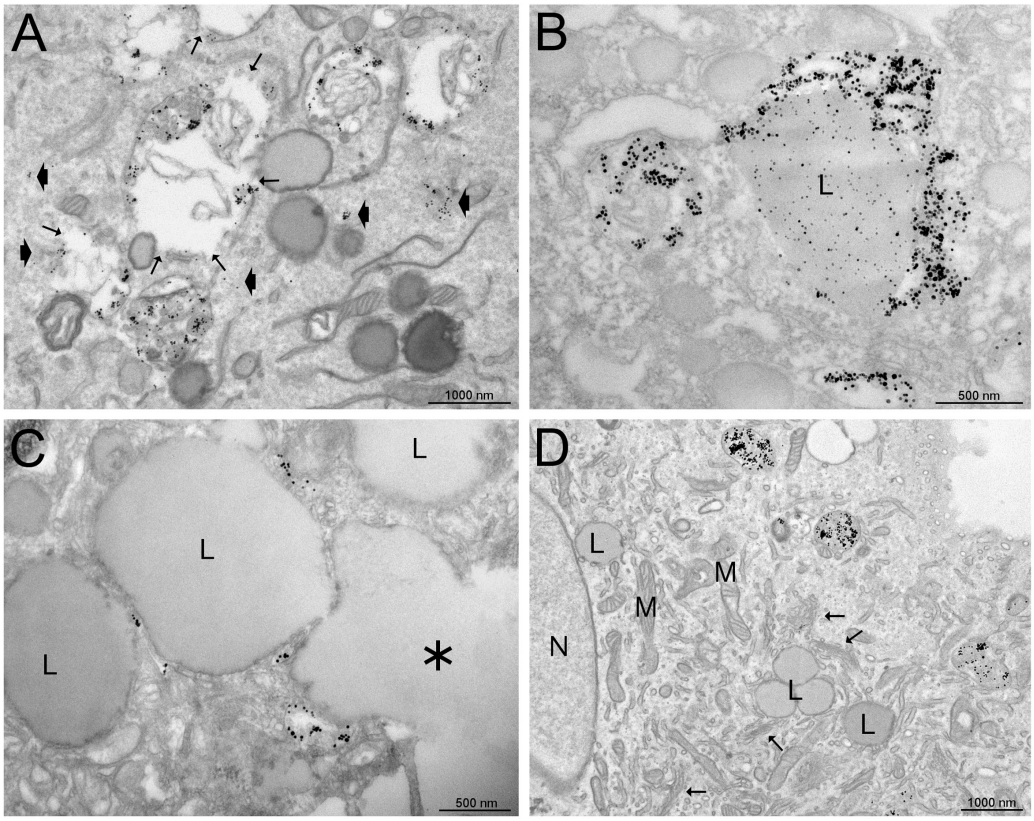

Figure 5: TEM images of adipocytes after PIONs-mediated SMHT. A) After hyperthermic treatment, some residual bodies containing PIONs appeared as damaged, with interruptions along their membranes (thin arrows), thus allowing the release of PIONs into the cytoplasm (arrowheads). B) Once free in the cytoplasm, some PIONs were found around and inside lipid droplets (L). C) Lipid droplets (L) approached the cell surface and were extruded (asterisk). D) 24 h after the hyperthermic treatment, a few lipid droplets of small size (L) were found in the cytoplasm, while mitochondria (M), endoplasmic reticulum and Golgi complexes (arrowheads) were well developed, demonstrating no cell damage and suggesting a high metabolic activity. N: cell nucleus.

Accordingly, the MTT assay and the quantitative determination of tumor suppressor p53 mRNA expression performed on adipocytes proved the safety of SMHT.

The histograms in Figure 6, A and B, show the percentage of cell viability under SMHT in comparison with control conditions (untreated cells subjected to AMF and cells treated only with PIOs but not exposed to AMF) both immediately after and 24 h after SMHT. No significant difference was noted in all cases compared to untreated cells at both time points.

Further confirmation of the safety of our approach was derived from quantitative determination of tumor suppressor p53 mRNA expression in adipocytes immediately after and 24 h post-treatment (Figure 6, C and D, respectively). This experiment was mandatory to provide information about cytotoxic and mutagenic

effects of SMHT treatment, as an impairment of p53 gene expression normally affects cell growth, programmed cell death/apoptosis and cellular senescence [21]. Our data confirmed that neither PIONs uptake nor AMF application and the combination of both (SMHT) affected significantly p53 expression, which is particularly relevant in view of a possible clinical translation of this therapeutic approach.

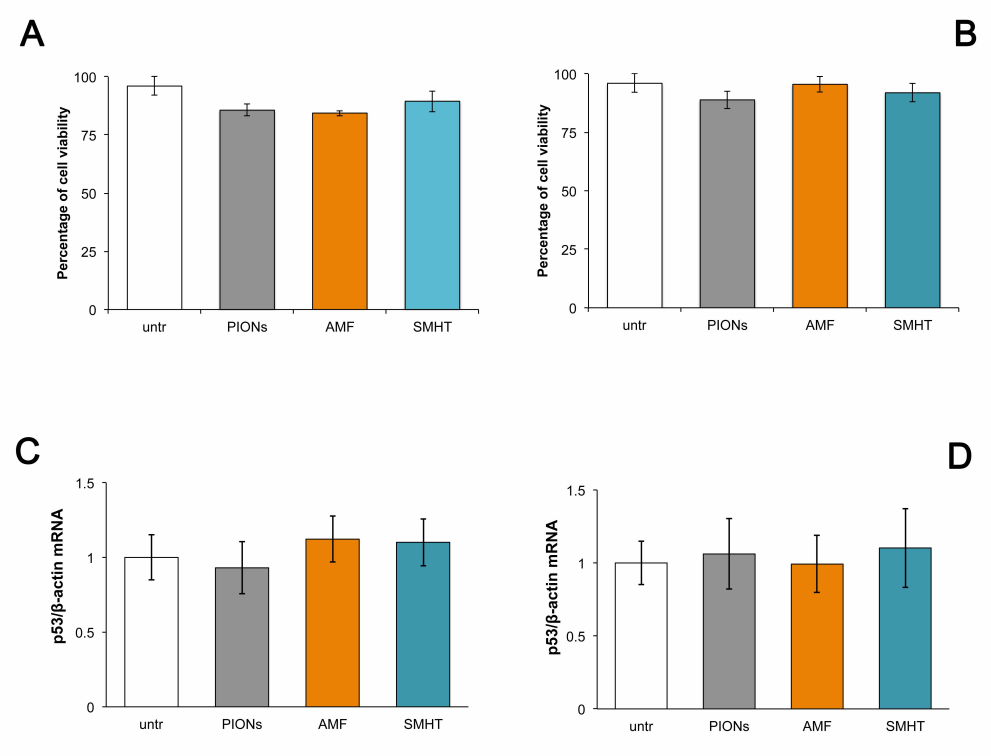

Figure 6: Effect of SMHT with PIONs on cellular viability. A) MTT assay performed immediately after and B) 24 h after hyperthermic treatment. The proportion of viable cells was referred to untreated adipocytes (100%). C) mRNA expression of p53 gene immediately after and D) 24 h after hyperthermia were obtained by qRT-PCR. Data were analyzed with the 2^(-ΔΔC_T) method [18] and normalized to untreated cells.

2.3.4. Lipolytic effect of SMHT in 3T3-L1 mature adipocytes

The effect of SMHT on the adipocyte metabolism was determined immediately after and 24 h after the SMHT.

The lipolytic effect of SMHT on adipocytes was firstly assessed using a light microscopy after staining the cells with Oil Red O (Figure 7, A-D). The lipid depletion was confirmed by the significant decreased absorbance values of Oil Red O- extracted stain corresponding to triglycerides amount (Figure 7E), as well as by the concomitant increase in glycerol content in the culture medium after SMHT (Figure 7F).

The absorbance of Oil Red O-extracted stain was measured by UV-vis spectroscopy. Eventually, to confirm the extrusion of glycerol outside the cells, we measured glycerol content in the medium by a colorimetric assay (Figure 7F).

Data by microscopy examination showed the effective reduction in the lipid content mediated by SMHT compared to the other treatments (Figure 7, A and C). Further analysis of triglyceride content showed significant decrease (> 65%) of the lipid droplets after the SMHT treatment compared to the controls (Figure 7E). Furthermore, as the decrease of lipid in adipocytes is mediated by the release of glycerol throughout the lipid droplets in the medium, the polyol content in the supernatants was measured by a colorimetric assay. The analysis of the supernatants showed an increasing in glycerol content in the medium up to 3.5 $\mu g\ mL^{-1}$ thus confirming its extrusion outside the cells (Figure 7F).

As showed by electron microscopy also light microscopy (Figure 8) revealed low lipid content up to 24 h after SMHT in the treated adipocytes. So the SMHT results in a prolonged lipolytic effect.

Beyond the evident lipolytic effect of SMHT, the results of these experiments suggested possible impact of this treatment on adipocyte metabolism that deserved more thorough investigation.

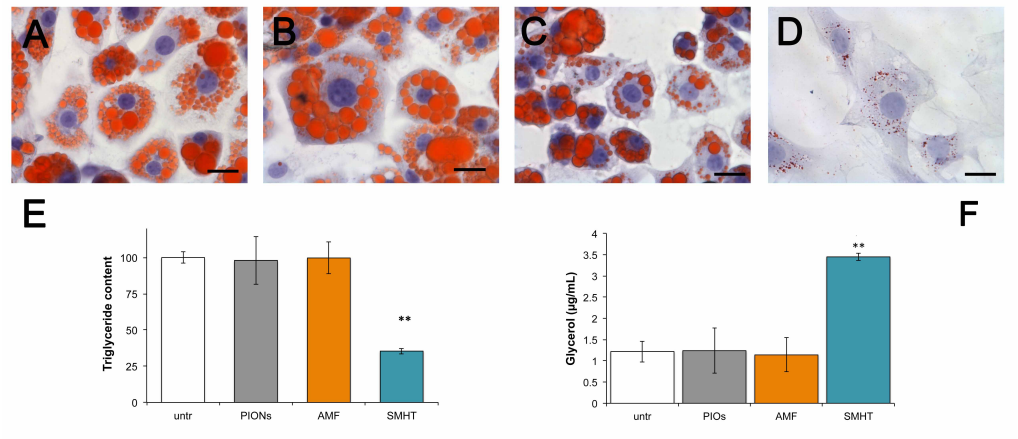

Figura 7: 3T3-L1 adipocytes subjected to hyperthermic treatment. SMHT hyperthermic treatment induces a visible reduction of lipid droplets in adipocytes (D) compared to the other treatment conditions, including A) control, B) PIONs without AMF, and C) AMF without PIONs. Intracellular lipid droplets were stained with Oil Red O and nuclei were stained with Eosin and visualized by light microscopy. Scale bar = 30 mm. The lipolytic effect was determined E) by assessment of the triglyceride content in adipocytes by fat extraction with isopropanol and spectrophotometric measurement of Oil Red O-stained adipocytes at 490 nm (data are referred to untreated sample, 100%). *P<0.01 *vs.* untreated; ^P<0.05 *vs.* PIONs and AMF and F) by measuring the amount of glycerol released in the medium after hyperthermia treatment using a colorimetric Glycerol Assay Kit providing a quantitative analysis of adipocyte content. *P<0.01 *vs.* untreated; ^P<0.05 *vs.* PIONs and AMF.

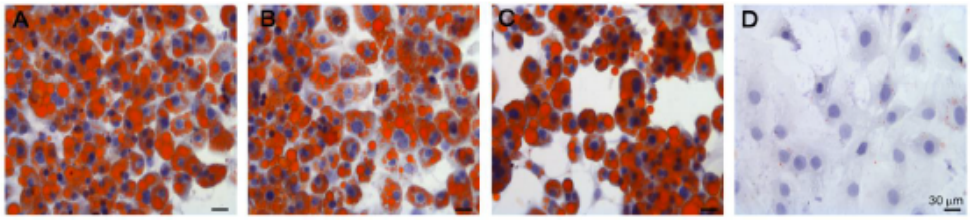

Figura 8: 3T3-L1 adipocytes 24 h after SMHT.Brightfield microscopy images (Oil Red O and hematoxylin staining) of control adipocytes (A), adipocytes incubated with PIONs (B), adipocytes exposed to AFM (C) and adipocytes 24h after SMHT.

2.3.5. SMHT effects on intracellular metabolism of triglycerides in 3T3-L1 adipocytes

To start getting insight into the molecular basis of the observed SMHT-induced lipolysis, we performed qRT-PCR analysis to assess the expression levels of key genes involved in lipid metabolism. We focused our attention on PPARγ and ATGL, as both genes play key roles in the adipolysis process [22, 23]. PPARγ mediates several processes among which the regulation of ATGL expression. ATGL is the limiting-step enzyme in the triglyceride metabolism, producing diacylglycerol, subsequently metabolized by hormone-sensitive lipase into glycerol and fatty acids. Therefore, ATGL plays a prominent role in triglyceride mobilization [24, 25]. In particular, due to the fact that ATGL is a key-enzyme in lipolysis deputed to triglycerides hydrolysis, it was investigated if the observed lipolytic effect observed after SMHT treatment was mediated by an overexpression of ATGL gene.

As shown in Figure 8, A and B, no significant differences were observed immediately after SMHT for both PPARγ and ATGL transcripts, compared with untreated, PIOs- and AFM-treated cells. This data also demonstrated that SMHT did not affect the status of cell differentiation as PPARγ is also a typical marker of mature adipocytes. Similar results were obtained 24 h after SMHT (Figure 7 E, F).

Lipid metabolism is a balance between adipolysis and adipogenesis [26]. Adipsin is acknowledged as a critical adipokine regulating adipogenesis trough the regulation of the acylation stimulating protein (ASP), a key mediator of adipose tissue triglyceride storage [27-29]. On this basis, we sought to investigate whether variations in adipsin expression had occurred as a cell attempt to compensate for lipid depletion (lipolysis), by promoting de novo triacylglycerol storage. As shown in Figure 8C, neither PIONs, AMF or SMHT significantly affected adipsin expression in comparison to untreated adipocytes.

These very interesting results suggested the involvement of a novel/alternative mechanism in the effective lipolysis observed.

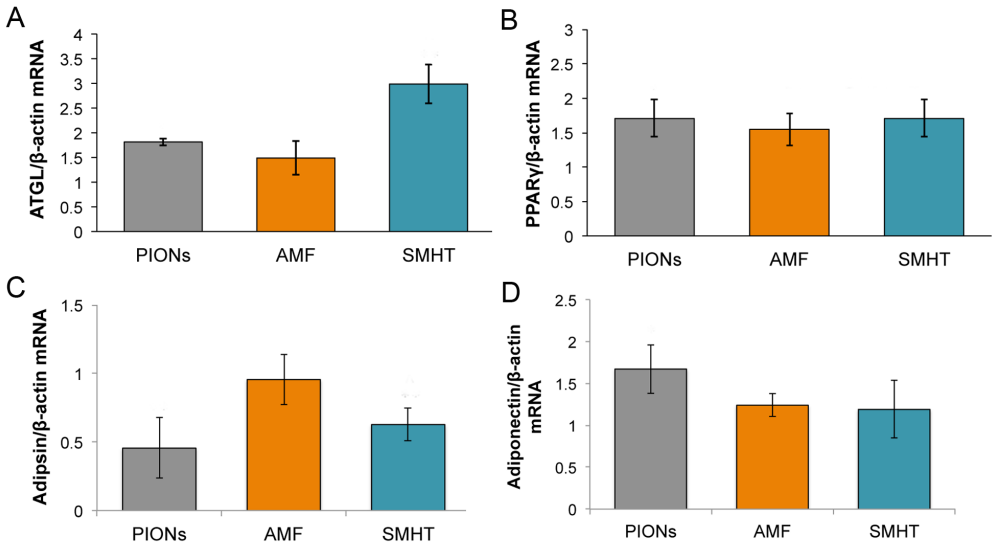

Figura 9: Immediately Effect of SMHT with PIONs on adipocyte metabolism. Relative mRNA expression of atgl, pparγ, atgl target genes in 3T3-L1 adipocytes. SMHT does not modify the status of differentiation of adipocytes (B), and the cellular metabolism (A, C, D). Gene expression was analyzed by quantitative real-time PCR. Data were analyzed with the 2-ΔΔCt method. Analysis were conducted in triplicate and statistical analysis were performed using the Mann Whitney U test. No signficant differences were found.

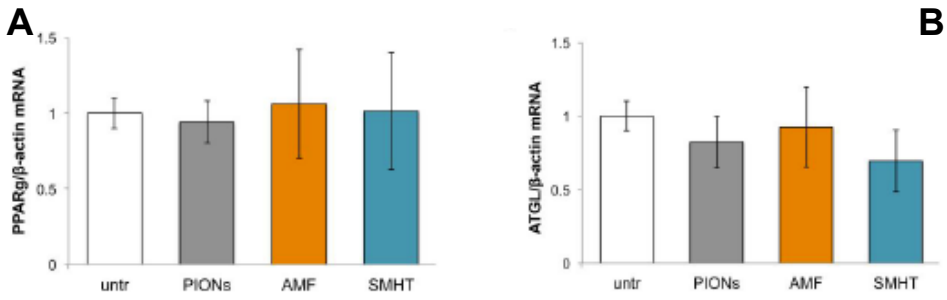

Figura 10: Effect of SMHT with PIONs 24 h after on adipocyte metabolism. Relative mRNA expression of pparγ, atgl target genes in 3T3-L1 adipocytes. SMHT does not modify the status of differentiation of adipocytes (A), and the cellular metabolism (B). Gene expression was analyzed by quantitative real-time PCR. Data were analyzed with the 2-ΔΔCt method. Analysis were conducted in triplicate and statistical analysis were performed using the Mann Whitney U test. No signficant differences were found.

2.4. Conclusions

Most life-threatening human pathologies, including cancer, diabetes mellitus, cardiovascular dysfunctions, and chronic inflammatory disorders are directly or indirectly caused by or associated to excess body weight. Thus, there is an urgent need to find out new solutions to rapidly and efficiently reduce the lipid components of adipose tissue using safe and physiologically mild approaches combined with healthy and balanced diet.

The results of our study suggested that targeting the energy storage of white adipose tissue with SMHT might be used as an innovative anti-obesity strategy promoving an anti-adipogenic effect.

The modulation of cellular metabolism in adipocytes takes advantage of the hyperthermic property of superparamagnetic iron oxide nanoparticles. Here we show that colloidally stable PIONs endowed with good heat capacity were taken up by mature adipocytes and released from endosomal compartmentalization into the cytoplasm upon application of an AMF, which results in PIONs accumulation in close proximity of lipid droplets. Free PIONs seem to preferentially migrate close to and even inside lipid droplets: this preference could be associated to the amphiphilic character of nanoparticle coating. SMHT triggers the disintegration of large lipid stores into minute droplets activating the metabolic function of the cell, which makes the metabolism and removal of triglycerides highly effective. This phenomenon does not induce cell damage probably because residual bodies do not contain lytic enzymes and/or membrane integrity is rapidly restored, similarly to the process of endosomal escape [30].

Interestingly, the observed lipolytic process is not accompanied by increased expression of ATGL, whose mRNA expression is normally elevated by peroxisome proliferator-activated receptor (PPARγ) agonists. This suggests that a pathway involving other than PPARγ and ATGL effectors may be involved in the lipolysis effect by SMHT and yet to be defined. Alternatively, one can hypothesize the occurrence of a "thermal stimulus" responsible for lipid extrusion to be further investigated. Moreover, mRNA expression of adipsin, the major adipokine released by adipose cells promoting triglyceride storage in adipocytes, was not upregulated

as a means to counteract the significant lipid loss, thus establishing a possible correlation with the prolonged (24 h) delipidated state of the SMHT-treated adipocytes. The latter observation further argues in favor of a lipolytic mechanism independent of the "canonical" events regulating the process.

This particular delipidation process has been recently investigated in detail in human adipocytes: it is an active process triggered by cell stress, and lipid droplets are extruded through micropores transitory forming in the plasmalemma, thus allowing cell structural preservation and viability [31].

Accordingly, adipocytes subjected to SMHT not only remain fully vital up to 24 h post-treatment, but also show well-preserved ultrastructural features and unaltered expression of genes involved in lipid metabolism and in cell differentiation process. This result is promising in view of the fundamental role of adipocyte differentiation in maintaining the cell commitment, preventing transcription and translation error rates and undesired signal deletions that increase the risk of neoplastic degenerations associated to obesity management.

Notably, the treatment results in a significant delipidation persisting, for at least 24 h, in the absence of cell death, damage or dedifferentiation. The biological reasons of such a rapid and massive lipolytic effect remain unclear. However our results clearly demonstrated that under controlled applied conditions SMHT can act as a mild controlled stress able to efficiently activate a physiological lipolytic process.

The success of this pioneering approach *in vitro* opens promising perspectives for the application of SMHT *in vivo* as an innovative safe and physiological mild approach against obesity. In view of a possible future translation of this therapeutic approach, we envisage that the effect of SMHT treatment of adipocytes might impact adipose hypertrophy and hyperplasia in overweight subjects thus affecting adipose tissue dysfunction and contributing in the prevention of cancer, T2D and cardiovascular diseases.

2.5. References

[1] Otto M.J., et al., The safety and efficacy of thermal lipolysis of adipose tissue via ultrasound for circumference reduction: An open label, single-arm exploratory study. *Lasers Surg Med.* 20 (2016) 734-741.

[2] Franco W., et al., Hyperthermic injury to adipocyte cells by selective heating of subcutaneous fat with a novel radiofrequency device: feasibility studies. *Lasers Surg Med.* 42 (2010), 361-70.

[3] Ito, K., et al., Development of microwave antennas for thermal therapy. *Curr Pharm Des.* 17 (2011) 2360-2366.

[4] D. Kim, D., et al., Bioavailability of nanoemulsified conjugated linoleic acid for an antiobesity effect. *Int. J. Nanomed.* 8 (2013) 451–459.

[5] Krentz, A. J., Evolution of pharmacological obesity treatment: focus on adverse side-effect profiles. *Diabetes Obes Metab.* 18 (2016) 558-570.

[6] Arner, E., et al., Adipocyte turnover: relevance to human adipose tissue morphology. *Diabetes* 59 (2010) 105–109.

[7] Renehan, A. G., et al., Adiposity and cancer risk: new mechanistic insights from epidemiology. *Nat. Rev. Cancer* 15 (2015) 484–498.

[8] H. B. Hubert, H. B., et al., Obesity as an independent risk factor for cardiovascular disease: a 26-year follow-up of participants in the Framingham Heart Study. *Circulation* 67 (1983) 968–977.

[9] A. H. Mokdad, A. H., et al., Prevalence of obesity, diabetes, and obesity-related health risk factors. *JAMA* 289 (2003) 76–79.

[10] Van Kruijsdijk, R. C. M., Obesity and cancer: the role of dysfunctional adipose tissue. *Cancer Epidemiol. Biomarkers Prev.* 18 (2009) 2569–2578.

[11] Pérez-Hernández, A. I., et al., Mechanisms linking excess adiposity and carcinogenesis promotion. *Front. Endocr.* 5 (2014) 1-17.

[12] P. Arner, P., et al., Dynamics of human adipose lipid turnover in health and metabolic disease. *Nature* 478 (2011) 110-113

[13] Jo, J., et al., Hyperthrophy and/or Hyperplasia: Dynamics of Adipose Tissue Growth. *PLoS Comput. Biol.* 5 (2009) e1000324. Doi:10.1371/journal.pcbi.1000324.

[14] P. Arner, P., et al., Lipolysis in lipid turnover, cancer cachexia, and obesity-induced insulin resistance. *Trends Endocrinol. Metab.* 25 (2014) 255–262.

[15] Duncan, R., et al., Regulation of lipolysis in adipocytes. *Annu. Rev. Nutr.* 27 (2007) 79–101.

[16] Rosen, E. D., Adipocytes as regulators of energy balance and glucose homeostasis. *Nature* 444 (2006) 847–853.

[17] Bernabucci, U., et al., Heat shock modulates adipokines expression in 3T3-L1 adipocytes. *J. Mol. Endocrinol.* 42 (2009) 139–147.

[18] Schmittgen, T. D., et al., Analyzing real-time PCR data by the comparative C_T method. *Nat. Prot.* 3 (2008), 1101-1108.

[19] Ramìrez-Zacarìas, J. L., et al., Quantitation of adipose conversion and triglycerides by staining intracitoplasmic lipids with Oil red O, *Histochemistry* 97 (1992), 493-497.

[20] Mahmoudi, M., et al., Assessing the in vitro and in vivo toxicity of superparamagnetic iron oxide nanoparticles. *Chem. Rev.* 112 (2012) 2323–2338.

[21] Bieging, K. T., et al., Unravelling mechanisms of p53-mediated tumour suppression. *Nat. Rev. Cancer* 14 (2014) 359–370.

[22] Kershaw, E. E., et al., PPARγ regulates adipose triglyceride lipase in adipocytes in vitro and in vivo. *Am J Physiol Endocrinol Metab* 6 (2007) 293.

[23] Zechner, R., et al. FAT SIGNALS—lipases and lipolysis in lipid metabolism and signaling. *Cell Met.* 15 (2012) 279-291.

[24] Duncan, R., et al., Regulation of lipolysis in adipocytes. *Annu. Rev. Nutr.* 27 (2007) 79–101.

[25] Arner, P., et al., Lipolysis in lipid turnover, cancer cachexia, and obesity-induced insulin resistance. *Trends Endocrinol. Metab.* 25 (2014) 255–262.

[26] Nielsen, T. S., et al., Dissecting adipose tissue lipolysis: molecular regulation and implications for metabolic disease. *J Mol Endocrinol.* 52 (2014) 199-222.

[27] Cianflone K., et al., Critical review of acylation-stimulating protein physiology in humans and rodents. *BBA* 1609 (2003) 127-143.

[28] Sniderman, A. D., et al., The Adipsin-ASP Pathway and Regulation of Adipocyte Function. *Ann Med.* 26 (1994) 389-393.

[29] J.C. Lo, J. C., et al., Adipsin Is an Adipokine that Improves β Cell Function in Diabetes. *Cell* 158 (2014) 41-53.

[30] Varkouhi A. K., et al., Endosomal escape pathways for delivery of biologicals. *J Controlled Release* 151 (2011) 220-8.

[31] Conti G., et al., The post-adipocytic phase of the adipose cell cycle. *Tissue Cell.* 2014 46 (2014) 520-6.

Appendix

Application of Thermotherapy to Glioblastoma

3.1 Introduction

3.1.1. Glioblastoma

"Gliomas are the most common type of primary brain tumour and are often fast growing with a poor prognosis for the patient. Their complex cellular composition, diffuse invasiveness and capacity to escape therapies has challenged researchers for decades and hampered progress towards an effective treatment" [1].

According to the World Health Organization system of classification and grading, Glioblastoma represents the most anaplastic tumour of astrocytic lineage-astrocytoma grade IV [2]. It is the most common and most aggressive, showing vascular endothelial proliferation, necrosis and very high cell density and atipias. Also the characterization of the distinct molecular genetic markers associated with the tumour has provided subclasses of glioma to be identified based on a molecular signature or gene expression patterns. This sub-classification allows the correlation of treatment effects or prognosis with molecular markers, so that patients can be more effectively selected for more appropriate therapies. The sub-classification has also contributed to the more detailed elucidation of components of molecular oncogenic pathways. For example which oncogenes are activated, such as the growth factor receptor (EGFR) involved with the migration of glioma cells throughout the central nervous system.

It is also important to underline the presence of the glioma stem cells, which are responsible for maintaining these tumours after therapy and repopulating tumours after gross total resection. These cells express markers that can be used to identify the cells that are capable of tumour formation when xenotransplanted and have a capacity for self renewal, clonogenicity and differentiation into a broad range of cell types. The most important marker of the cancer stem cell is the CD133 [3].

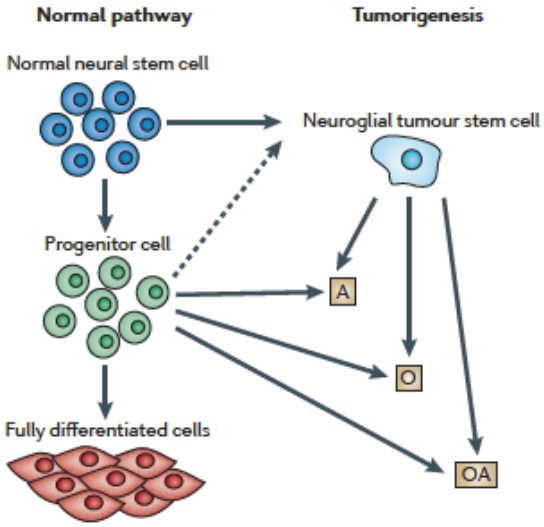

Figure 1: Stem cell differentiation and tumorigenesis [1].

3.1.2 SPIONs as contrast agents in MRI

The use of SPIONs as contrast agents for MRI was associated with substantial increases in diagnostic sensitivity and specificity [4]. The aim of their use is visualizing molecular characteristics of physiological or pathological processes in living organisms before they manifest in form of anatomic changes.

MRI offers several advantages over alternative techniques, including lack of irradiation, possibility to generate 3D images, excellent spatial resolution with optimal contrast within soft tissues and a very good signal-to-noise ratio. Paramagnetic (e.g. gadolinium) and superparamagnetic (e.g. SPIONs) compounds can be used as MR contrast agents. While the paramagnetic species enhance the signal in T1-weighted images resulting in positive contrast, magnetic nanoparticles provide strong signal enhancement in T2-weighted images (negative contrast), owing to a different contrast mechanism [5].

Contrast agents may be used for identifying specific biomarkers. Ideally, the biomarkers should be abundantly and only expressed on the desired cell types. Furthermore, disease-specific biomarkers should be clearly different form healthy status. To identify the specific biomarker SPIONs would be composed of two components: 1) the magnetic iron oxide core represents the imaging component and 2) the attached molecules represent the targeting or affinity component..

In case of tumours a contrast can be observed between tissues with and those without having captured superparamagnetic iron oxide nanoparticles, owing to a difference in the precession frequency of water protons in proximity of paramagnetic nanodipoles (Figure 11).

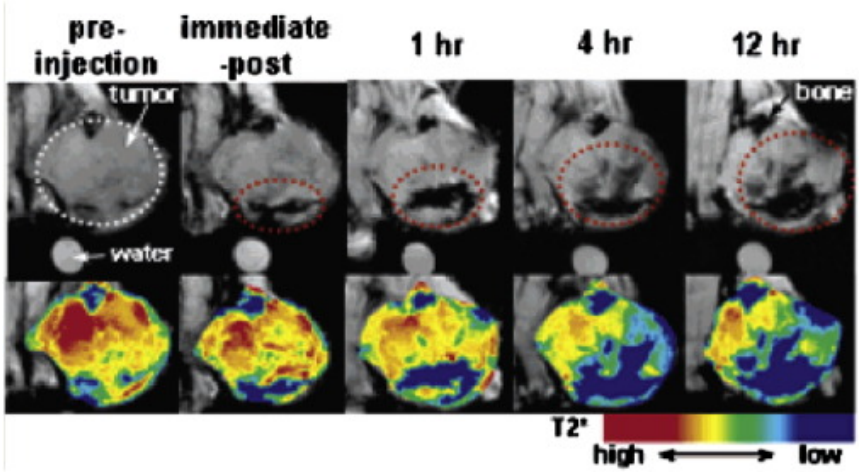

Figure 2: iron oxide nanoparticles for early detection of cancer [6].

3.1.3. SPIONs as theranostic agents

"Theranostic" is defined as the capacity of combining diagnosis and therapy into a single agent [7]. "Theranostic agents" allow obtaining more specificity and more sensibility in the therapeutic diagnosis and prognosis.

Nanotechnology has offered an unprecedented opportunity to design "nanotheranostic agents" that can act as therapeutic and contrast agent combining therapy and diagnosis. These nanoparticles possess unique optical or magnetic properties that could be combined with the loading of therapeutic agents allowing for the conjugation of a second or third functionality, a feature that encourages the formation of an all-in-one nanosystems with comprehensive features.

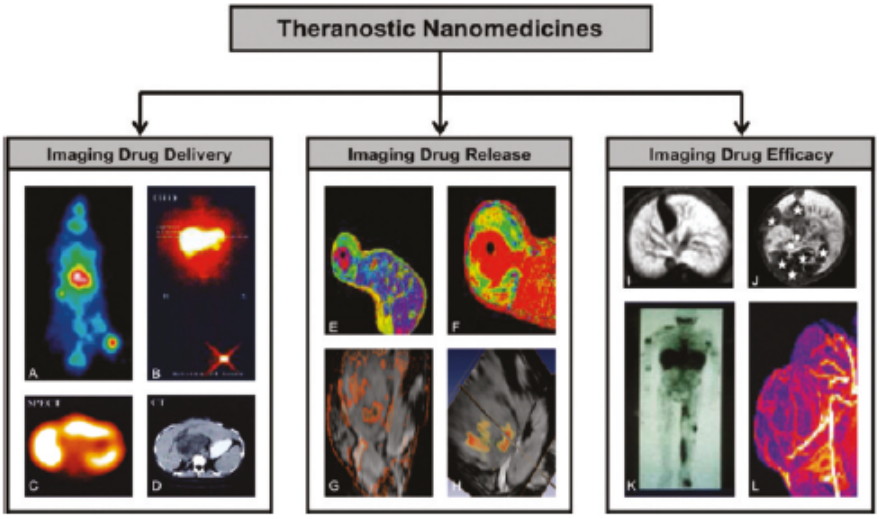

Figure 3: Application of theranostic nanomedicine formulation [7].

3.1.4. Targeting nanoparticles

The real challenge in nanomedicine is represented by the possibility of realizing a therapeutic agent with maximum specificity and sensibility. It means develop a nanoparticle capable of recognizing the sick site showing its effect preferentially in this site with a real reduction of side effects. For this purpose designing suitable functionalized nanoparticles is a general procedure claim.

To increase to probability of achieving the target the first requirement is a long-circulating effect. As the macrophages recognize the nanoparticles as "hosts" and remove them from the blood circulation is necessary to realize macrophage-evading nanoparticles. Furthermore, long-circulating particles escape from macrophages

could accumulate where the capillaries have open fenestrations and vascular abnormalities such as in tumour or in obesity cases where the endothelial barrier is perturbed by inflammatory or other processes.

The design of such "stealth " nanoparticles requires the consideration of a multitude of physico-chemical and physiological factors, affecting circulation time [8].

Generally the surface protection by a barrier of hydrophilic groups prevents the opsonin adsorption and therefore avoids the macrophage recognition. Among several molecules, linear dextrans, Polyethylene glycol (PEG) and their derivates are widely used in order to improve the circulation lifetime and bioavailability and decrease their immunogenicity, renal clearance rate and dosing frequency. PEG has been shown to be the most effective polymer for suppressing protein adsorption. It is the α,ω–dihydroxyl derivate of polyethylene oxide and is a flexible polymer, hydrophilic (but also soluble in some organic media), not biodegradable and easily excreted from living organisms by physiological routes. The optimal molecular weight varying between 2000 and 5000 Da and its functional end-groups are available for derivatization leading to numerous possibilities for covalent attachment.

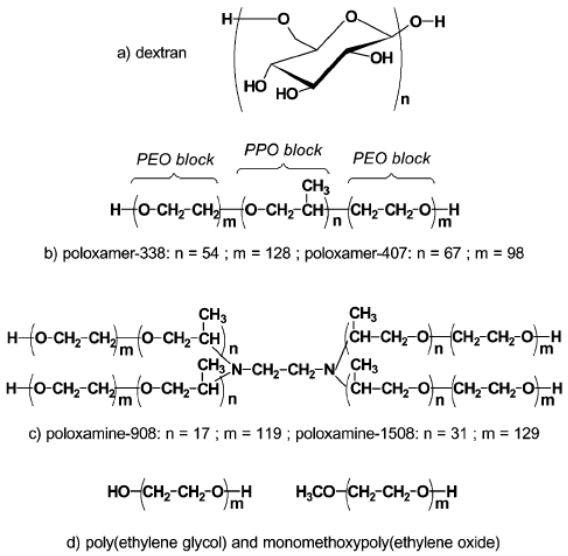

Figure 4: macromolecules used as hydrophilic coating for monuclear phagocyte system-evading nanoparticles [9].

Ligand conjugation is the second requirement for active targeting. To enhance the capability of long-circulating nanoparticles to be uptaken from target cells , the surface of nanoparticles has to be modified with ligands that specifically bind to the

receptors present on the target cells, by molecular recognition processes involving antibody-antigene interactions. Among these ligands, often recurring are oligosaccharides, oligopeptides, folic acid, antibodies and their fragments.

Due to the unique specificity of monoclonal antibodies for their molecular counterparts and to the possibility to produce immunoglobulins for almost every known marker receptor, this class of proteins is usually considered the preferred choice for active targeting and great effort has been devoted to the development of antibody-functionalized nanocarriers.

Therefore, for tumour targeting, folic acid, antibodies or peptides could be grafted to PEGylated nanoparticles in order to take advantage of the frequent overexpression of the specific receptors onto the surface of human cancer cells. Interestingly, nanoparticles conjugated with antibodies appeared to interact more efficiently with their receptors than free antibodies.

However, antibody coupling has at least two drawbacks: 1) the overall size of the antibodies (typically into the range 15-20 nm), which cause particles to diffuse poorly through biological barriers, and 2) their immunogenicity, i.e. the property of being able to elicit an immune response within an organism.

For this reason, the coupling of small non-immunogenic ligands to polymeric carriers has been also investigated.

3.1.5. GE11 Peptide

Targeting may be essential for efficiency mediated cell-binding of shielded nanoparticles and enhanced nanoparticles uptake by receptor-mediated endocytosis or related uptake pathways.

Epidermal growth factor (ErbB1, EGFR) is a typical receptor used for targeting tumour cells and is overexpressed by glioblastoma cells. Various EGFR binding molecules have been explored as targeting ligands, including recombinant EGF protein, EGFR binding antibodies and peptides. Among all these ligands the enriched phage clone encoding the amino acid sequence YHWYGYTPQNVI (designated as GE11) was described as the best efficient. "Competitive binding assay and Scatchard analysis revealed that GE11 peptide bound specifically and efficiently to EGFR with a dissociation constant of 22 nM, but with much lower mitogenic activity than with EGF. The peptides were internalized preferentially into EGFR highly expressing cells, and they accumulated in EGFR overexpressing tumor

xenografts after i.v. delivery *in vivo*. In conclusion GE11 is a potentially safe and efficient targeting moiety for selective drug delivery systems mediated through EGF" [10].

The PEGylation reduces the complement activation (innate immune system), improves solubility, reduces the interaction with blood cells and serum proteins, provides a better biocompatibility and prolongs blood circulation times [11].

3.1.6. Aim of the work

Currently there is no an efficient cure and only very limited progress has been made in the control of the glioblastoma course. Thus, the need for effective therapies is great. In particular this involves the drug delivery across the blood-brain barrier. Beyond molecular targeting of a specific cellular signalling pathway, more complex tumour-associated processes such as cell migration, immunosuppression or angiogenesis could also be targeted.

Several studies proved that heat shock produces apoptosis on cancer cells resulting in tumour reduction.

Even if the use of my previous PIOs was mainly dedicated to adipose tissue, I reasoned that changing the synthesis procedure could be also exploited to obtain a more efficient heating mediator and to induce a hyperthermic effect in glioblastoma cells as described in Chapter 1.

The aim of the present study was to investigate the effect of applying intracellular superparamagnetic hyperthermic treatment (SMHT) in reducing the mass tumour as a novel strategy to counteract glioblastoma and the cell migration.

It is worth noting that, similarly to many other nanoparticles, SPIONs surface may be functionalized and their distribution controlled by targeting strategies, thus focusing the hyperthermic treatment preferentially in the unhealthy cells.

So I decided to functionalize IONs with the GE11 peptide targeting EGF receptor of glioblastoma cell line to have an active targeting so to induce the thermotherapy preferentially on the cancer cells reducing side effects. In fact for glioblastoma targeting GE11-$PEG_{12}NH_2$ peptide has been shown to mediate sequence-specific binding of model nanoparticles to EGFR expressing cells and remarkably increased uptake activity.

3.2. Materials and Methods

3.2.1. Cell cultures

U87-MG cell line (purchased by ATCC Manassas, VA), was cultured in Eagle's Minimum Essential Medium (EMEM) with 10% of Fetal Bovine Serum (FBS), 1% of a mix of penicillin/streptomycin 1:1 and 1% of L-glutamine 200 mM, in 25 cm^2 plates and incubated at 37°C in humidified air with 5% CO_2. Medium and L-glutamine were purchased by Sigma-Aldrich (Italy), while serum and antibiotic mix were acquired by GIBCO Life Technologies (USA). When at confluence, cells were treated with trypsin-EDTA 1% (GIBCO Life Technologies, USA), harvested and centrifuged at 1200 rpm for 5 min. The supernatant was discarded and cells pellet was resuspended in 1 ml of complete medium, placed in 75 cm^2 plates and incubated at 37°C and 5% of CO_2 until 80% confluence was detectable. EGFR expression in U87MG cells was determined using flow cytometer FACSCanto (BD biosciences) with a primary anti-EGFR antibody and an anti-□FITC antibody secondary (millipore).

3.2.2. GE11 Solid-phase Synthesis

GE11-$PEG_{12}NH_2$ peptide is generated by standard Fmoc-Solid phase assisted synthesis (SPS). SPS offers a way to synthesize precisely defined oligomer structures. The SPS can be carried out manually with an overhead shaker using microreactors with polyethylene filters for vacuum filtration. The amount of resin depends on the determined resin loading and of the scale size (1/L [mmol/g] x scale size [mmol] = resin amount [g]). Approximately 10 μmol of resin correlate with approximately 20 mg of yield.

I always followed a repetitive synthesis cycle:

- Coupling (60 min).
- Washing (3× DMF, 3× DCM).
- Kaiser's Test (1).
- Deprotection (2).
- Washing (3× DMF, 3× DCM).
- Kaiser's Test.

A 2-chlorotrityl chloride resin is used as solid support. The Resin was firstly loaded in a syringe reactor and swelled with DCM for 20 min. Coupling of the Fmoc protected amino acids is performed with a fourfold excess (based on the quantity of free amines) whilst an identical excess of HOBt and PyBOP is used for preactivation. DIPEA is added with an eightfold excess (also related to free amines). HOBt and PyBOP are dissolved in 5 mL of DMF/g of resin and the (artificial) amino acids are dissolved in 5 mL of DCM/g of resin. The corresponding amount of DIPEA is added, the solutions are mixed for preactivation and added to the resin.

Coupling, as well as deprotection are verified by testing for free amines qualitatively using Kaiser's test. If the result is unsatisfying the previous coupling or deprotection step is repeated.

For the GE11PEG$_{12}$NH$_2$ I followed this procedure:

1. Considering resin loading and desired synthesis scale size, take the required amount of preloaded 2-chlorotritylchloride resin and transfer into the corresponding reactor.
2. Swell the resin for 30 min with 10 mg/mL DCM.
3. Synthesize the GE11 peptide by sequential coupling and deprotection of Fmoc-L-Ile-OH, continue with Fmoc-Val-OH, Fmoc-L-Asn(Trt)-OH, Fmoc-L-Gln(Trt)-OH, Fmoc-L-Pro-OH, Fmoc-L-(Thr)-tBu-OH, Fmoc-Tyr(tBu)-OH, Fmoc-L-Gly-OH, Fmoc-Tyr(tBu)-OH, Fmoc-Trp(BOC)-OH, Fmoc-L-His(Trt)-OH and end with Fmoc-Tyr (t-Bu)-OH.
4. Continue with the synthesis at the free amine by coupling Fmoc-dPEG12-NH2 using the standard coupling conditions.
5. Dry the peptide on high vacuum for 30 min
6. Prepare a clevage cocktail (3) for cleaving the resin from the acid labile linker
7. Apply 10 mg/mL of cleavage solution to resin for 90 min at RT and collect it afterwards.
8. The resin is washed afterwards three times with 10 mg/mL resin of TFA.
9. Allow the combined solutions to evaporate to 1mL and to precipitate in a dropwise manner into a 50 mL of ice cold precipitating solution (4).
10. Centrifuge for 20 min (4000 g, 4°C), discard the supernanant and dry the precipitate under nitrogen (N2) stream.

11. Dissolve the obtained product in size exclusion running buffer and purify it by Size Exclusion Chromatography (SEC).

12. Take the product containing fractions, and pool them into a tared 15 mL tube, then snap freeze and lyophilize.

The GE11PEG$_{12}$NH$_2$ peptide were purified with Sephadex G10 size exclusion chromatography (SEC) medium and characterized with MALDI_TOFL instrument. At the end the obtained HCl salt of the oligomer was stored at -20 °C.

Fmoc and Boc-protected α-amino acids were purchased from Iris Biotech, Marktredwitz, Germany) and Fmoc-N-amido-dPEG12-NH2 from Quanta Biodesign, Powell, Ohio, USA. DCM, N,N-Dimethylformamide (DMF), DIPEA. 1-Hydroxybenzotriazole (HOBt). Benzotriazol-1-yl-oxy tripyrrolidinophosphonium hexafluorophosphate (Pybop®) were purchased from Multisyntech GmbH, Witten, Germany.

3.3. Results and Discussion

Taking the advantage of the SPS I obtained a novel GE11-$PEG_{12}NH_2$ oligomer charatecterized by a well-defined chemical structure as described in Figure 5.

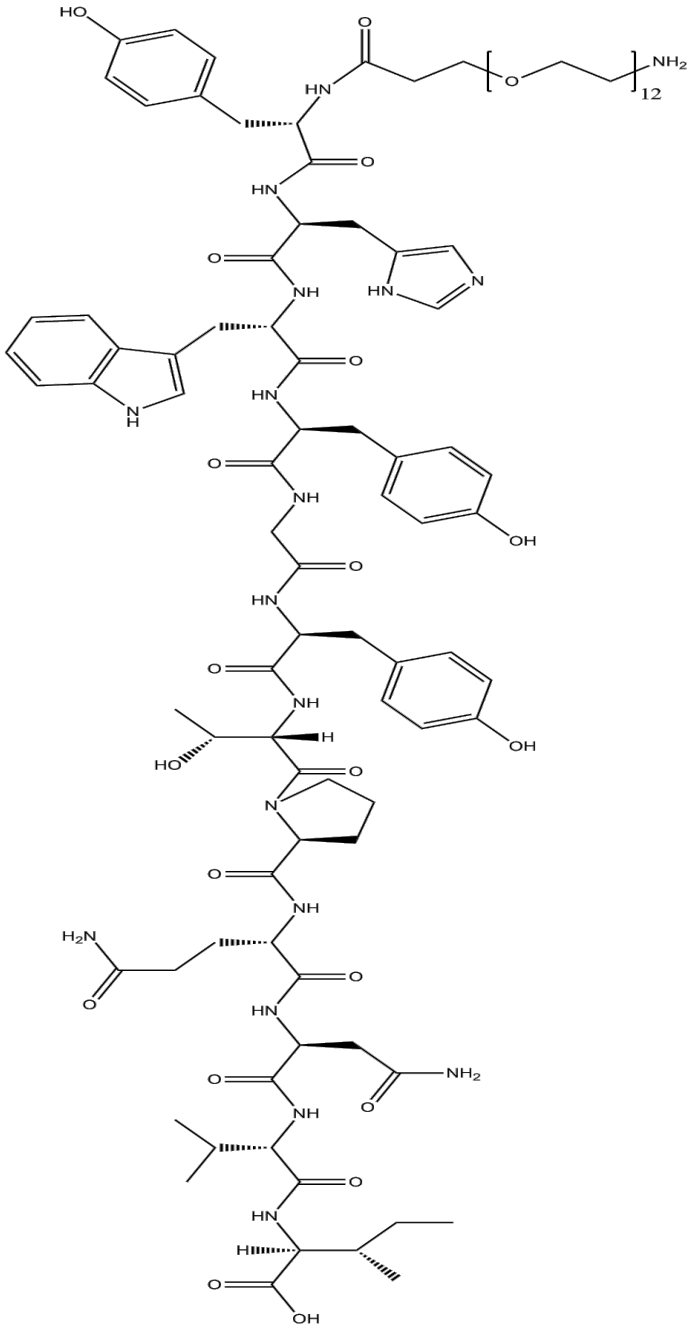

Figure 5: Chemical structure of GE11 peptide conjugated with $PEG_{12}NH_2$.

The high yield of the synthesis and the purity of the obtained oligomer were confirmed by Mass Spectroscopy (Figure 6). The final molecular weight of the above described $GE11PEG_{12}NH_2$ oligomer was determined as 2141,3 Da.

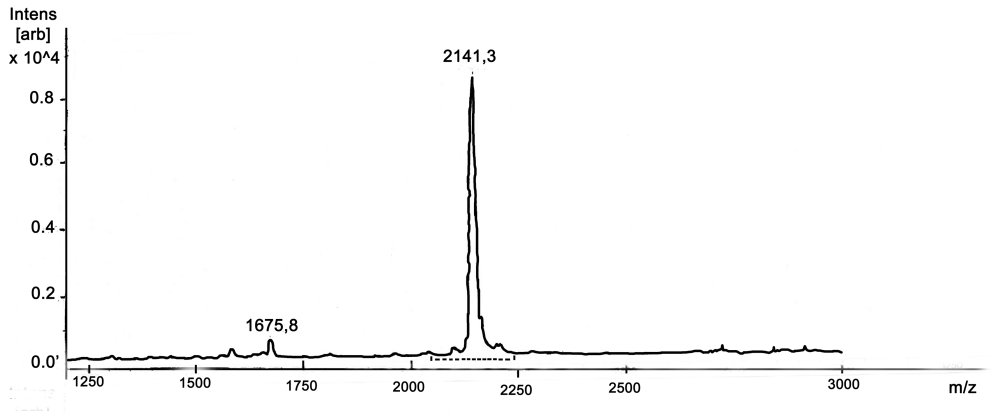

Figure 6: Mass Spectrum of GE11-$PEG_{12}NH_2$.

3.4. Conclusions

Nowadays the need for an efficient therapy of the glioblastoma disease is great. The prognosis for the patients with glioblastoma is always poor and the treatments are ineffective and often very toxic.

Thus, there is an urgent need to find out new solutions to rapidly and efficiently reduce the tumour mass using safe specific and physiologically mild approaches.

Thermotherapy was described as a very innovative and efficient treatment that colud be combined with surgery. However is necessary to develop a suitable, stable and efficient heating mediator.

Unfortunately, as described in Chapter 1 IONs obtained until now need to be optimized realizing a best efficient heating mediator.

However, the result of the SPS suggested that once obtained suitable IONs, they could be immediately functionalized with the GE11 peptide realizing an active targeting thermotherapy for glioblastoma. In fact the glioblastoma cells were 95% positive for the EGF receptor and the GE11 peptide is the best ligand for this receptor.

This approach might be used as an innovative anti-glioblastoma strategy. The death of the glioblastoma cells might take advantage of the hyperthermic property of superparamagnetic iron oxide nanoparticles hypothesizing a "thermal stimuls" responsible of the "killing effect".

Notably, the studies described in literature, the promising thermotherapy effect and the need of realizing an efficient therapy suggest continuing with the synthesis optimization of the IONs, with the functionalization with the GE11 peptide targeting selectively the glioblastoma cell line.

3.5. References

[1] Westphal, M., et al., The neurobiology of gliomas: from cell biology to the development of therapeutic approaches, *Nat. Rev. Neurosci.* 12 (2011) 495-508.

[2] Louis, D. N., et al., The 2007 WHO classification of tumours of the central nervous system. *Acta Neuropathol.*, 114 (2007), 97-109.

[3] Singh, S. K., et al., Identification of human brain tumour initiating cells, *Nature* 432 (2004) 396–401.

[4] Corot, C., et al., Recent advances in iron oxide nanocrystal technology for medical imaging. *Adv Drug. Delivery Rev.* 58 (2006) 1471-1504.

[5] Semelka, R. C., et al., Contrast agents for MR Imaging of the liver, *Radiology* 218 (2001) 27-38.

[6] Huh, Y. M., et al., In vivo magnetic resonance detection of cancer by using multifunctional magnetic nanocrystals, *J Am Chem Soc* 127 (2005) 12387-12391.

[7] Lammers, T., et al., Theranostic nanomedicine, Acc. Chem. Res. DOI:10.1021/ar200019c.

[8] Kawai, N., et al., Effect of heat therapy using magnetic nanoparticles conjugated with cationic liposomes on prostate tumour in bone, The Prostate, 68 (2008), 784-792.

[9] Mornet, S., et al., Magnetic nanoparticle design for medical diagnosis and therapy. *J. Mater. Chem.* 14 (2004) 2161-2175.

[10] Li, Z., et al., Identification and characterization of a novel peptide ligand of epidermal growth factor receptor for targeted delivery of therapeutics. FASEB J. 19 (2005) 1978–1985.

[11] Knop K, et al., Poly(ethylene glycol) in drug delivery: pros and cons as well as potential alternatives. *Angew Chem Int Ed Engl* 49 (2010) 6288-6308.

3.6. Notes

(1) The Kaiser's test solutions is based on 80% (w/v) phenol in EtOH; 5% (w/v) ninhydrin in EtOH; KCN/pyridine (2 mL of 1 mM KCN in 98 mL of pyridine). 2% 1 mM KCN (v/v) in pyridine.

(2) Fmoc-deprotection solution is composed of 20% (v/v) piperidine/DMF.The Capping solution: 80/15/5 (v/v/v) DCM/MeOH/DIPEA.

(3) The Cleavage cocktail: 95/2.5/2.5 (v/v/v) trifluoro acetic acid (TFA)/triisopropylsilane (TIS)/dH_2O.

(4) The Precipitating solution: 1/1 (v/v) methyl *tert*-butyl ether (MTBE)/n-hexane.

General Conclusions

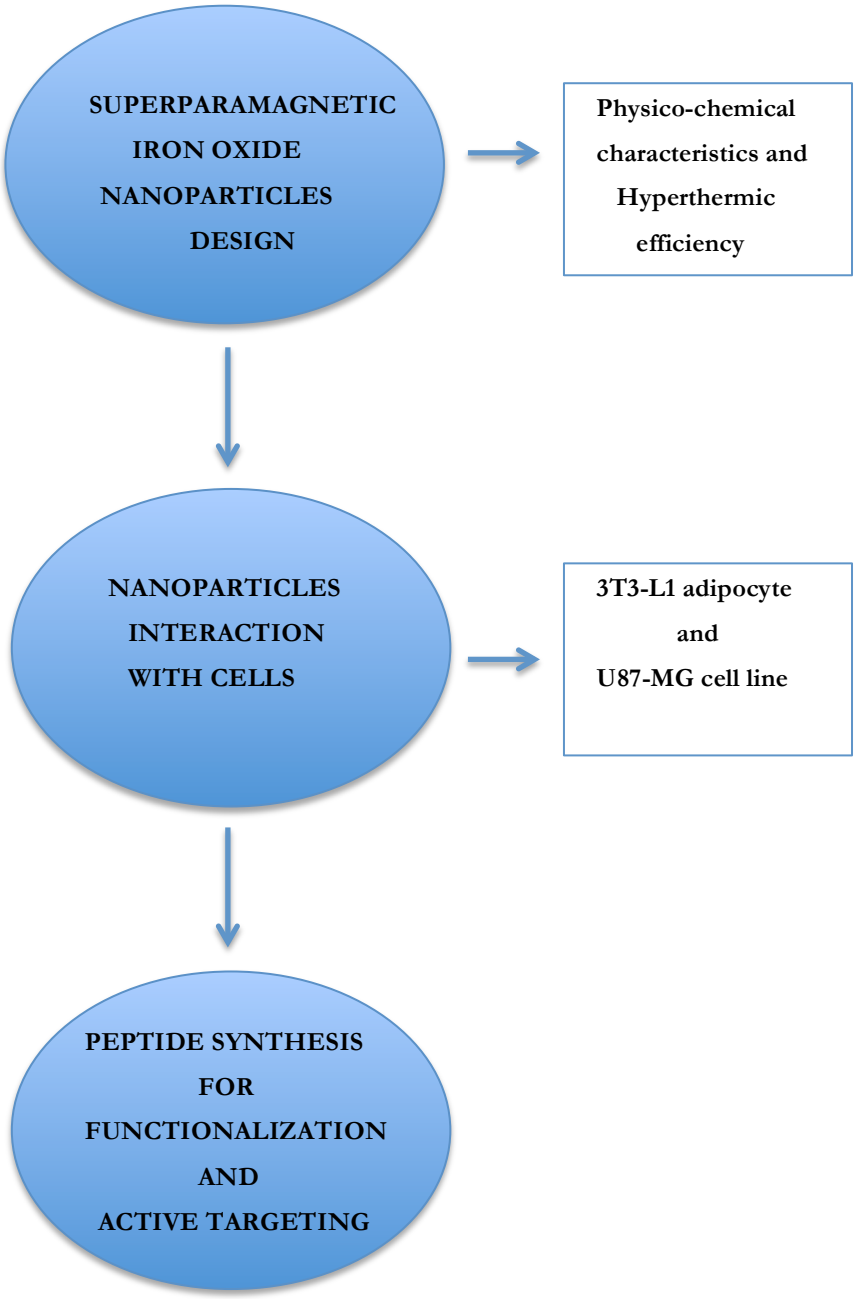

During my PhD I have studied the therapeutic potential of Hyperthermia mediated by SPIONs in two different *in vitro* cellular models of two relevant hyperproliferative diseases: 3T3-L1 adipocytes for obesity (Chapter 2) and U87-MG for Glioblastoma (Chapter 3).

Given the nanostructure of these SPIONs, there is a broad range of options in their construction and functionalization of their surface, which makes it possible to endow them with multiple and specific properties.

However the efficacy and safety of nanoconstructs must be preserved and validated by in vitro studies in order to avoid side effects, in view of the development of therapeutic approaches.

Based on these considerations, in the present thesis I have taken advantage of SMHT to address the following issues of biomedical relevance:

- In Chapter 1 I have presented the possibility to synthesize efficient SPIONs as heating mediator. My results suggested that only one type of SPIONs, namely PIONs, were able to induce heat when subjected to AMF and only them could provide heat capacity sufficiently suitable for the utilization as heating mediators in our *in vitro* model. These PIOs were stable in physiological milieu for at least 6 months and were covered by an amphiphilic polymer realizing nanoparticles that could be functionalized with peptides for active targeting.
- In Chapter 2, I have carried on *in vitro* studies on adipocyte cell line, using PIONs as heating mediators whereby SMHT causes an impact on the adipocytes triglyceride metabolism. The results of our study suggested that targeting the energy storage of white adipose tissue with SMHT might be used as an innovative anti-obesity strategy promoving an anti-adipogenic effect. Notably, the treatment results in a significant delipidation persisting, for at least 24 h, in the absence of cell death, damage or dedifferentiation. The biological reasons of such a rapid and massive lipolytic effect remain unclear.
- In Chapter 3, I have presented the SMHT application on glioblastoma cell line. This study is very preliminar so I could only show the perspective of this application. In the first step I tried to synthesyze a more efficient SPIONs-heating mediator, but the bad heating results suggested to optimize the synthesis procedure. However I realized a very efficient oligomer characterized by the sequence GE11PEG$_{12}$NH$_2$ as targeting agent for the glioblastoma cell line. Once obtained the suitable IONs they could be immediately functionalized with the GE11 oligomer realizing an active targeting thermotherapy for glioblastoma. In fact the glioblastoma cells were 95% positive for the EGF receptor and the GE11 peptide is the best ligand for this receptor. This approach might be used as an innovative anti-glioblastoma strategy. The death of the glioblastoma cells might take advantage of the hyperthermic property of superparamagnetic iron

oxide nanoparticles hypothesizing a "thermal stimuls" responsible of the "killing effect".

In conclusion, we were able to produce very promising heating mediator for SMHT with high efficiency of heating, stability and good safety for the surrounding microenvironment of therapeutic agents in case of adipocyte cell line. The success of this pioneering approach *in vitro* opens promising perspectives for the application of SMHT *in vivo* as an innovative safe and physiological mild approach against obesity and the studies described in literature, the promising thermotherapy effect and the need of realizing an efficient therapy suggested us to continue with the synthesis optimization of the IONs, with the functionalization with the GE11 peptide targeting selectively the glioblastoma tumour.